

SWIRLING FLOW OF MAXWELL FLUID WITH BIOCONVECTION PHENOMENON

By

MARYAM EHSAN ABBASI



NATIONAL UNIVERSITY OF MODERN LANGUAGES

ISLAMABAD

October, 2023

Swirling Flow of Maxwell Fluid with Bioconvection Phenomenon

By

MARYAM EHSAN ABBASI

MS Mathematics, National University of Modern Languages, Islamabad, 2023

A THESIS SUBMITTED IN PARTIAL FULFILMENT OF
THE REQUIREMENTS FOR THE DEGREE OF

MASTER OF SCIENCE

Mathematics

To

FACULTY OF ENGINEERING & COMPUTING



NATIONAL UNIVERSITY OF MODERN LANGUAGES ISLAMABAD

© Maryam Ehsan Abbasi, 2023



THESIS AND DEFENSE APPROVAL FORM

The undersigned certify that they have read the following thesis, examined the defense, are satisfied with overall exam performance, and recommend the thesis to the Faculty of Engineering and Computing for acceptance.

Thesis Title: Swirling Flow of Maxwell Fluid with Bioconvection Phenomenon

Submitted By: Maryam Ehsan Abbasi

Registration #: 13 MS/MATH/F20

Master of Science in Mathematics
Title of the Degree

Mathematics
Name of Discipline

Dr. Awais Ahmed
Name of Research Supervisor

Signature of Research Supervisor

Dr. Sadia Riaz
Name of HOD (MATH)

Name of HOD (MATH)

Dr. Muhmmad Noman Malik
Name of Dean (FEC)

Signature of Dean (FEC)

October , 2023

AUTHOR'S DECLARATION

I Maryam Ehsan Abbasi

Daughter of Muhammad Ehsan Abbasi

Registration # 13 MS/Maths/F20Discipline Mathematics

Candidate of **Master of Science in Mathematics (MS Maths)** at the National University of Modern Languages do hereby declare that the thesis "**Swirling Flow of Maxwell Fluid with Bioconvection Phenomenon**" submitted by me in partial fulfillment of MS Maths degree, is result of my own research except as cited in references. This thesis has not been submitted or published earlier. I also solemnly declare that it shall not, in the future, be submitted by me for getting any other degree from this or any other university or institution. I also understand that if evidence of plagiarism is found in my thesis at any stage, even after the award of a degree, the work may be canceled and the degree revoked.

Signature of Candidate

Maryam Ehsan Abbasi
Name of Candidate

October, 2023

Date

ABSTRACT

Title: Swirling Flow of Maxwell Fluid with Bioconvection Phenomenon

Dynamics of non-linear fluid viscoelastic fluid with bioconvective properties is the core concern of the present thesis. There are many applications for non-linear fluids can be found in industry. Such as production of polymer and plastic sheets etc. encounter these types of the fluid flow. Therefore, in this era the scientists put their efforts to investigate the flow and thermal transport features of non-Newtonian fluids. These types of the liquids include time-dependent, time-independent and viscoelastic type fluids. The viscoelastic type of fluid exhibits both viscous and elastic effects. The deformation tensor for viscoelastic non-linear fluids is used in empirical model called "Maxwell fluid model". This model is the part of the present study in swirling type flow phenomena which is induced by rotating cylinder. Both Dufour and Soret effects are also included in the energy equation for the thermal analysis. The governing equations are changed into a set of nonlinear ordinary differential equations with appropriate flow ansatz. In MATLAB bvp4c, the converted nonlinear ordinary differential boundary value problem is solved with suitable boundary conditions. The impacts of dimensionless factors on velocity, temperature, concentration, and concentration of microorganisms are visually depicted in graphical abstract using a comparison of constant wall temperature (CWT) and prescribed surface temperature (PST).

TABLE OF CONTENTS

1	Introduction	1
2	Literature Review	3
	2.2 Research Gap.....	18
	2.3 Research Objective.....	18
3	Preliminaries	19
	3.1 Basic Definitions.....	19
4	Flow of Maxwell Fluid engender by Torsional Motion of Cylinder	37
	4.1 Introduction.....	37
	4.2 Mathematical Formulation.....	37
	4.3 Numerical Solution.....	41
	4.4 Presentation of Results.....	42
5	Swirling Flow of Maxwell Fluid with Bioconvection Phenomenon subject to Soret and Dufour Effect	57
	5.1 Introduction.....	57
	5.2 Mathematical Formulation.....	57
	5.3 Method of Solution.....	61
	5.4 Results and Discussion.....	62
6	Conclusions and Future Work	77
	References	78

LIST OF TABLE

TABLE NO.	TITLE	PAGE
1	Numerical data of $-\theta'(0)$ for different values of Re , β_1 , Pr , and $M = 0$.	56
2	Numerical values of $f'(1)$ and $g'(1)$ for various Re in case when $\beta_1 = M = 0$	76

LIST OF FIGURES

FIGURE NO.	TITLE	PAGE
3.1	Maxwell Model	22
3.2	Kelvin-Voigt	22
3.3	Standard Linear Solid (SLS) or Zener Model	23
3.4	Laminar Flow	26
3.5	Turbulent Flow	26
3.6	Pattern of Bioconvection	30
4.1	Flow Diagram	38
4.2(a)	Variation in $f'(\eta)$ for increasing values of Re	44
4.2(b)	Variation in $f'(\eta)$ for increasing values of β_1	45
4.2(c)	Variation in $f'(\eta)$ for increasing values of M	45
4.2(d)	Variation in $f'(\eta)$ for higher values of M	46
4.3(a)	Variation in $f(\eta)/\eta$ for various values of Re	46
4.3(b)	Variation in $f(\eta)/\eta$ for various values of M	47
4.4(a)	Change in $g(\eta)$ for increasing values of β_1	47
4.4(b)	Change in $g(\eta)$ for increasing values of Re	48
4.4(c)	Trend of $g(\eta)$ for higher values of M	48
4.4(d)	Change in $g(\eta)$ for increasing values of M	49
4.5(a)	Change in $\theta(\eta)$ for increasing values of Re	49
4.5(b)	Change in $\theta(\eta)$ for increasing values of Pr	50
4.5(c)	Change in $\theta(\eta)$ for increasing values of Pr	50
4.6(a)	Change in $\phi(\eta)$ for increasing values of β_1	51
4.6(b)	Change in $\phi(\eta)$ for increasing values of Le .	51
4.7(a)	Change in $F'(\xi)$ for increasing values of β_1	52
4.7(b)	Change in $F'(\xi)$ for increasing values of M	52
4.8(a)	Change in $G(\xi)$ for increasing values of β_1	53
4.8(b)	Change in $G(\xi)$ for increasing values of M	53
4.9(a)	Change in $\Phi(\xi)$ for increasing values of M .	54

4.9(b)	Change in $\Phi(\xi)$ for increasing values of β_1	54
4.10(b)	Change in $\Theta(\xi)$ for increasing values of β_1	55
4.10(a)	Change in $\Theta(\xi)$ for increasing values of M	55
5.1	Geometry of the problem	58
5.2(a)	Variation in $f'(\eta)$ for increasing values Re	65
5.2(b)	Variation in $f'(\eta)$ for increasing values β_1	65
5.2(c)	Variation in $f'(\eta)$ for increasing values M	66
5.3(a)	Variation in $g(\eta)$ for increasing values of Re	66
5.3 (b)	Velocity component $g(\eta)$ for increasing values of M	67
5.4 (a)	Change in $\theta(\eta)$ for increasing values of β_1	67
5.4 (b)	Temperature profile $\theta(\eta)$ for increasing values of Sr	68
5.4 (c)	Change in $\theta(\eta)$ for higher values of Du	68
5.4 (d)	Change in $\theta(\eta)$ for increasing values of Le	69
5.4 (e)	Variation in $\theta(\eta)$ for more values of M	69
5.4 (f)	Variation in $\theta(\eta)$ for large values of Pr	70
5.4 (g)	Trend of $\theta(\eta)$ for increasing values of Re	70
5.5(a)	Magnetic field impact on in $\phi(\eta)$	71
5.5 (b)	Behaviour of $\phi(\eta)$ for increasing values of Re	71
5.5 (c)	Behaviour of $\phi(\eta)$ for more values of Sr	72
5.5 (d)	Behaviour of $\phi(\eta)$ for the values of Du	72
5.6 (a)	Trend of $h(\eta)$ for more values of M	73
5.6 (b)	Trend of $h(\eta)$ for increasing values of Re	73
5.6 (c)	Trend of $h(\eta)$ for higher values of Sb	74
5.6 (d)	Variation in $h(\eta)$ for higher values of Pe	74
5.6 (e)	Variation in $h(\eta)$ for various values of Lb .	75
5.6 (f)	Variation in $h(\eta)$ for higher values of N_g	75

LIST OF SYMBOLS

α_1	Thermal diffusivity
A_1	Rivlin-Ericksen tensor
β	Maxwell Number
C_P	Specific Heat Capacity
C_w	Cylinder's surface Concentration
D_B	Mass Diffusivity
D_u	Dufour Number
S_r	Soret number
E	Represents Cylinder's constant torsion
J	Mass flux
J_1	Density of Current
Le	Lewis number
M	Magnetic parameter
Pe	Peclet number
Pr	Prandtl number

q	Heat Flux
Re	Reynolds Number
S	Extra Stress Tensor
Sb	Bioconvection Schmidt number
Sc	Schmidt number
T_w	Cylinder's surface Temperature
$\frac{d}{dt}$	Material derivative
ρ	Density of Fluid
λ_1	Relaxation time
$\frac{D}{Dt}$	Oldroyd derivative
μ	Viscosity

ACKNOWLEDGEMENT

Firstly, In the name of Almighty Allah, the most Merciful and Compassionate, All the worship and honor is for Him, Who always helped me to stick to the right path and always provided me the courage and strength to complete my degree with hard work and dedication.

I would like to convey my heartfelt thanks and admiration to Dr. Awais Ahmed, my highly esteemed supervisor. Throughout my academic journey, he provided me with invaluable aid and inspiration to ensure the timely completion of all tasks assigned to me. His constant support and expertise helped me successfully navigate every aspect of writing my thesis. As a result, I will always cherish his selfless contributions and keep him in my prayers.

I want to express my gratitude to the Department of Mathematics, National University of Modern Languages, Islamabad, for providing me with a diverse range of learning methods through their dedicated staff and faculty members.

My gratitude goes out to my parents and siblings, whose aid, motivation, and unwavering backing have been invaluable. Their unwavering assistance has been my backbone, as their prayers have kept me going up to this point.

Maryam Ehsan Abbasi

DEDICATION

My family and supervisor have played a crucial role in my dissertation work. I'm especially grateful to my parents, who instilled in me the values of working hard with dignity and humility and never giving up on hope and faith. Equally important has been to my Supervisor, who serves as a true mentor for me, and continues to inspire, uplift, and provide guidance so i can complete my research within the designated time frame.

CHAPTER 1

INTRODUCTION

The branch of continuum science, fluid dynamics, revolves around investigation the flowing characteristics of fluids, whether they are Newtonian or non-Newtonian. Due to its versatile characteristics, it finds extensive use in both natural sciences and engineering fields having the variety of applications in engineering mechanisms that can be made using the flow produced by rotating and stretchable boundaries, the subject of fluid dynamics has attracted a lot of investigation attention. The thermal investigation in viscous liquid across a constantly extending surface within a fluid medium that is otherwise quiescent has attracted a large amount of interest over the years. There have been numerous manufacturing processes that have been developed in response to this problem, including hot rolling, wire drawing, metal extrusion, crystal growth, continuous casting, and the creation of glass fiber, and paper.

Crane [1] was the first to discover the analytical solution for an incompressible viscous fluid flowing on a stretching sheet in a boundary layer. After that, numerous researchers conducted research on the flow pattern over expanding surfaces. [2,4,5] Investigated heat transfer mechanism and flow in viscous fluids on nonlinear stretching sheets. The thin film of an unstable Maxwell fluid was the subject of analysis in the study conducted by Dandapat *et al.* [3]. Analyzing the flow and temperature fields on a moving surface, Tsou *et al.* [6] utilized analytical and experimental methods. The purpose was to examine the various characteristics of the flow. Sprague and Weidman [7] investigated how an extremely flexible cylindrical sheet affects the surrounding flow. Tahir *et al.* [10] conducted an analytical study of three-dimensional MHD viscous flow in a rotating frame. A novel mathematical model was employed to scrutinized the characteristics of (MHD) flow of non-linear Maxwell fluid over a

flexible, heat-conducting spinning disc, which was examined by Khan *et al.* [11]. Ahmed *et al.* [13] conducted a study on the flow of thin films of Maxwell fluids over rotating discs, and explored the impact of non-linear thermal radiation.

Choi *et al.* [17] researched the behavior of Maxwell liquid with upper-convected rate of change as it flows through a two-dimensional steady state in a porous surface channel, without any volume changes. The study investigated the fluid's flow properties. To study, the transfer of flow, mass with heat on a stretched surface, various studies have been conducted [19], [9], [12]. Madhu *et al.* [24] investigated the non-Newtonian Maxwell nanofluid flow on a stretched sheet with radiation of heat. The objective of Javed *et al.* [25] was to investigate how the flow of an axially symmetric Casson liquid that passes through a stretched cylinder is affected by heat production and absorption, which arise due to the twisting motion of the cylinder that causes the flow.

Microbes, possessing a higher density than water, generally exhibit upward movement, leading to bioconvection. Bioconvection can be initiated when the upper-layer of a suspension becomes unstable due to the sedimentation of micro-organisms, resulting in its collapse towards the bottom. The bioconvection process is sustained by swimming microorganisms that return upwards. Bioconvection finds diverse applications across various industries. Bioconvection has emerged as a significant factor in a range of fields, including biotechnology, environmental systems, modern engineering, and biological systems. Essentially, it refers to the movement of fluid at a macroscopic level caused by the activity of microorganisms such as algae and bacteria, which generate density gradients in the fluid. Riaz *et al.* [31] theoretically analyzed how the transmission of concentration and thermal affects MHD natural convection in fluid flows with viscoelastic properties. A comprehensive review of all research conducted in this field between 1992 and 2005 was carried out by Hill *et al.* [33].

Pedley *et al.* [35] developed a model that specifically examines the linear instabilities that occur within a uniform mixture of gyrotactic microorganisms. Bioconvection can be induced by gyrotactic bacteria in nanofluids, as reported in the research conducted by Kuznetsov *et al.* [42]. The bioconvection phenomenon has been analyzed through various theoretical and practical studies [41-47].

CHAPTER 2

LITERATURE REVIEW

In recent times, there has been a significant focus on the rheological behavior of non-linear fluids along a stretched sheet in the boundary layer. Many researchers have been focused on the boundary layer issues related to surfaces that are both stretched and rotating for the last few decades. This is because the engineering and industrial production industries benefit from a variety of applications. The flow phenomena in rotating cylinder applications are determined by the cylinder's direction to the flow and the rotational axis. In the branches of physics and fluid mechanics, the boundary layer denotes the part of a fluid in a specific zone where viscosity significantly influences its movement. Furthermore, it is an area of the flow field where the fluid deforms with a relative velocity.

The following literature is reviewed for the present study. Crane [1] was the first to discover the analytical solution for an incompressible viscous fluid flowing on a stretching sheet in a boundary layer. Wang [2] researched closed form solutions for all Prandtl numbers of integer multiples of $1/2$, as well as the vertical free convection problems. Dandapat *et al.* [3] examined the movement of an incompressible second-order fluid triggered by the expansion of a level flexible area, utilizing the principles of boundary layer theory. Skin friction reduces when the elastic factor increases. The heat transmission analysis in this flow indicates that, for a particular Prandtl number, the temperature at a site increases with increasing elastic parameter while the wall and ambient temperatures remain constant.

Vajravelu [4] the features of heat transmission and flow inside a viscous fluid on a nonlinear stretching surface were examined using analysis. This study focuses on the flow that results from a stretching wire entering a still fluid through an orifice. A viscous fluid's heat transport and flow characteristics across a non-linearly expanding sheet are studied. The

governing equations that regulate flow and heat transport are partly separated using a similarity transformation different from that used in the linearly stretched sheet problem. (However, as a specific instance, the answers for the linearly extending sheet issue may be achieved). The Runge-Kutta integration technique of 4th order is used to compute the non-linear system of differential equations for the velocity field f and the temperature field considering the coefficient's variation. Numerical data for the heat energy transfer parameters are presented through the use of a table and graphs.

Fang and Yao, [5] studied a viscous flow over a cylinder with torsional and stretching motion. For the entire value of the flow Reynolds number, the Navier-Stokes equation has an approximate and unique solution. As pointed out by the findings, increased Reynolds number leads to quicker decrease in velocity, thereby causing the fluid flow to penetrate more deeply into the encompassing fluid. An algebraic pattern of decline, with final velocity being zero is perceived in all velocity profiles. Tsou *et al.* [6] studied the boundary layer's flow and temperature fields on a moving surface using both analytical and experimental approaches. The study aimed to analyze both turbulent and laminar conditions. Analytical results exist for both the profiles of temperature and flow within the boundary-layer and the coefficients related to surface friction and heat transfer.

The effect of a cylinder's torsional motion on a three-dimensional flow was investigated by Sprague and Weidman [7]. An extremely cylindrical sheet that is flexible and performs pure torsional motion has its surrounding flow examined. The issue is controlled by the torsional Reynolds number $R = \gamma a^2 / \nu$, the kinematic viscosity of the fluid, and the axial rate of rotation are denoted by ν and γ , respectively, referring to the radius of the cylinder. A slight transverse flow develops in the meridional plane due to the primary flow's axial pressure gradient, which is an intriguing aspect of the problem. This motion's axial component manifests as a wall jet. The comprehensive numerical findings obtained throughout the broad range of Reynolds numbers $10^{-2} \leq R \leq 10^6$ are shown and contrasted with the higher values of Reynolds number asymptotic for parameters of the shear stress and the radially transported flow.

A thermally layered medium incorporates an exponentially elongated sheet experiencing suction and MHD (the term magnetohydrodynamics is made up of three words:

magneto, hydro, and dynamics, which stand for magnetic field, water, and movement, respectively) boundary layer flow and heat transmission was presented by Mukhopadhyay, [8]. It is necessary to convert the momentum and energy equations, which are partial differential equations, into highly nonlinear ordinary differential equations, and this can be done using appropriate transformation techniques. The shooting approach is employed to obtain analytical results for these equations. The surface experiences an enhanced heat transmission rate due to the thermal-stratification. A flow velocity declined as the magnetic parameter boostup, because the rate of heat transfer at the surface increases. The uneven flow of a narrow bi-viscosity liquid layer across a spontaneously stretched two-dimensional surface has been examined. Analytical outcomes are provided for the entire Navier-Stokes equations and the equation of continuity, as well as nonlinear free surface boundary conditions. In other terms, analytical solutions are achieved when both the governing and boundary equations are nonlinear PDE. It is proposed to solve the flow issue using the methods of single perturbation and characteristic functions. The results reveal that the original quasi film thickness produces planar film after a long period of time, whereas the initial planar film remains flat. Furthermore, bi-viscosity liquid thins the quicker than Newtonian liquid.

It has been observed by Takhar *et al.* [9] that the flow and transmission of heat in a spinning fluid under a magnetic field over a stretching surface is investigated. With the assistance of implicit finite difference and difference-differential procedures, equations that govern non-similar flow yield a numerical solution. The Nusselt number will decrease and the coefficient of skin friction will rise when the magnetic field is directed in the x-axis. As a result, when the rotational parameter increases, the Nusselt number decreases, but when the skin friction coefficients increase, Nusselt numbers increase. There is an increase in Nusselt numbers, with Prandtl numbers.

Tahir *et al.*[10] investigated rotating frame three-dimensional MHD viscous flow analytical treatment. The flow is caused by a sheet being uniformly stretched in the x-direction. An ordinary differential equation is formed by the conversion of partial differential equation by using the method of perturbation to produce the results in analytical form. To see how the various factors affect the velocity profiles, graphs are presented. A brand-new mathematical pattern was proposed by Khan *et al.* [11]to examine the properties of transportation in magneto hydrodynamic (MHD) flow of a Maxwell fluid through a stretched rotating disc that is convectively heated. To manage the temperature of the fluid's surface, a

simple isothermal model is implemented for both uniform and non-uniform operations. It is investigated how non-linear thermal radiative heat flux affects thermal transport properties.

The flow of bio magnetic Maxwell fluid in a three-dimensional boundary layer across a flat horizontal surface that is linearly extended in two mutually perpendicular directions was examined by Murtaza *et al.* [12]. The basic principles of both magneto-hydrodynamics (MHD) and ferro-hydrodynamics (FHD) have been utilized. Heat generation and absorption's impact has been considered. The work is theoretical, and it makes use of both approximation and numerical methods. By contrasting the numerical findings with those of earlier research that was described in the literature accessible, the correctness of the numerical approach has been verified. The results have been shown visually. The effects of several research factors, including the magneto-hydrodynamic and ferro-magnetic characteristics, Deborah number, stretching ratio, and heat production, are explored.

Ahmed *et al.*[13] conducted research on the flow of Maxwell nanofluid over a rotating disc while subjected to various factors such as temperature, electromagnetic field, and nonlinear thermal radiation. The research utilized the Buongiorno model to explore specific nanofluid properties, including Brownian motion and thermophoresis. The primary focus was on investigating the temperature field in nanofluid thin film flow and the distribution of nanoparticle volume fractions within it. The process for obtaining numerical solutions to the simplified differential system utilizes the bvp4c method of finite differences, which is applied in a simplified format. Varied estimations of relevant physical parameters have been used to disclose numerical outcomes for thickness of film, energy transport rates, velocity of flow, concentration and temperature distributions, hence producing a consequential outcome. This study shows that when the magnetic number of the film increases, the thickness of the film decreases. Furthermore, the impact of thermophoresis and thermal-radiation factors on fluid temperature is worthwhile. Brownian motion and Schmidt number are found to reduce solute concentration.

Wang [14] investigated that surface is stretched in a rotating fluid. An important parameter that affects the solution to the governing non-linear differential equations is the rotation to stretching rate ratio. Perturbation solutions can be contrasted with direct numerical integration for accurate calculations, regardless of whether the problem is of a small or large

λ . Using a Maxwell viscoelastic based micropolar, the non-linear behavior was investigated by Waqas *et al.* [15]. The stretching sheet is also saturated with a porous substance. In order to obtain the ordinary differential equations of the velocity, temperature profiles, and concentration, a number of similarity variables were used in this analysis. To investigate heat transmission features for radial stagnation point flow, the thermal case study was conducted by Rehman *et al.* [16]. The study assumed that the heated viscous nanofluid is in a linear twisting cylinder and analyzed the arrangement of rotating cylinders and radial stagnation point flow. A total of three potential factors are outlined in the study: the amount of nanoparticles in the nanoparticle volume, the amount of nanoparticles per unit volume, and the Wang's Reynolds number.

The flow properties of a upper-convected Maxwell fluid through a porous surface channel in a two-dimensional steady state with no changes in volume were studied by Choi *et al.* [17]. They managed to find a solution for injection and suction that resembles a Newtonian fluid. A Newtonian flow solution for suction and injection was developed. In the range of Deborah and Reynolds values $0 \leq Re \leq 30$ and $0 \leq De \leq 0.3$., the power series and numerical integration solutions for the Maxwell fluid perfectly match each other. This study also finds that, when Reynolds numbers are constant, viscoelasticity impacts velocity field in the same way that inertia impacts velocity profiles in a Newtonian fluid. As well as the injection flow of the Maxwell fluid, the self-similar solution is also applied.

Ahmed *et al.* [18] created a numerical representation for an electrically charged Maxwell fluid flow that which occurs between a central parallel stretchy spinning disc that is held at a fixed distance from the other disc which is electrically charged. The temperature-dependent thermal conductivity of an axially magnetic field is considered in the pressure and heat transmission study. Both discs' stretching and rotation speeds are believed to be different. For flows pressure and temperature domain, the impact of effective parameters are investigated for the same and opposite rotation direction. The stretching action improved the basic flow pattern occurring between the discs, which are one of the key physical implications of this work.

Seddeek [19] studied how heat exchange is affected by radiation and the coefficient of thermal diffusion when a stretching sheet with varying heat flow is present. A numerical solution is generated for a variety of values of the variable diffusion coefficient, radiation

parameter, temperature parameter, and Prandtl number in order to obtain a numerical solution. It has been reported that Salleh [20] has studied the heat exchange and steady flow across a stretchable surface.

The flow of a viscous liquid in a two-dimensional stagnation-point has been studied by Mahapatra [21]. The velocity of the liquid has a direct proportionality to the distance from the stagnation point, and it moves across a flat surface that is constantly deformed at a fixed rate. As a matter of fact, it has been shown in this study that boundary layers form whenever a velocity of stretching is lower than a free-stream velocity, and when the extending velocity exceeds a free stream velocity, an upturned boundary layer form. To analyze the temperature gradient in the boundary layer, it involves maintaining a constant temperature on the surface while inspecting the thermal dynamics within this thin layer. The stable and completely developed solutions for stratified flows on horizontal and inclined planes of a fluid having non-Newtonian shear-thinning characteristics are one of the phases described by Picchi *et al.* [22]. Concurrent and counter-current arrangements that work practically are discussed.

Gangadhar *et al.* [23] performed a theoretical investigation on the flow, heat, and mass transmission properties of a Maxwell fluid in a porous channel immersed across a stretched surface with viscous dissipation and embedded within a stretched surface with a stretched surface. An effective analytical approach, the spectrum relaxation technique, is used to provide the numerical solution for the set of modified equations generated from the physical pattern of the flow. Following that, mathematical results are produced in order to analyze the convergence and reliability of the suggested approach. The effects of various flow regulating factors encountered in the problem are handled. All of the results of the numerical technique are shown in graphs and tables to analyze the several generated parameters. As the porosity of the medium strengthens, significant changes occur such as the increase in shear stress at surface and decrease in energy transportation rates.

The study of non-Newtonian Maxwell nanofluid boundary layer flow on a stretched sheet with radiation of heat was analyzed by Madhu *et al.* [24]. The visco-elastic Maxwell model is utilized to explain the dynamics of non-linear fluids in order to explain their behavior. The resolution of the paired nonlinear ordinary differential equations is carried out with assistance from the variational finite element method. For various values for regulating flow parameters, the flow properties, the properties of heat transmission, and the volume percentage

of nanoparticles are all investigated and described in depth. Studying both systems, gas to liquid and liquid to liquid, the exact solution is utilized to analyze how the rheological properties affect the shear-thinning liquid's multiple flow properties. While the non-Newtonian fluid is often the heavier stage in gas-to-liquid systems, it is typically the lighter point in liquid-to-liquid systems (for example, waxy oil with aqueous phase lubrication) (e.g., two-phase flow of natural gas and pure oil). This research can be applied to a variety of situations and is not limited to thin non-Newtonian layers.

Heat production and absorption have an effect on axially symmetric flow of Casson liquid across a stretchable cylinder. Javed *et al.*[25] scrutinized flow generated by twisting motion of a cylinder. Using the built-in-shooting method, it is possible to solve these equations numerically using the built-in-shooting technique. The controlling physical issue is represented by a series of linked nonlinear ordinary differential equations. Several factors can be assessed and studied in relation to the physical effects of whirling velocity, temperature, coefficient of friction, and heat transmission rate, among others. The magnitude of axial skin friction rises with increasing Reynolds number and magnetic parameter, but the local Nusselt number decreases with increasing Casson parameter, heat production or absorption, and magnetic parameter. Previously published data is also provided in the ultimate situation for comparison.

The issue of flow infringing radially on a cylinder at a linearly twisting stagnation point was considered by Weidman, [26]. There was also the problem of stagnation-point flow on a cylinder rotating in a linear direction, which was also discussed. The problem was governed by a non - dimensional twisting rate and a Reynolds number. Multiple radial and azimuthal velocity profiles can be produced for different Reynolds values, providing an overview of wall shear stresses across the range of R . Despite the weak nature of axial wall shear stress, the parameter $g'(1)$ for azimuthal wall shear stress holds significant importance. Conversely, the axial wall shear stress parameter $f'(1)$ is still considered quite weak.

Mabood *et al.* [27] conducted research indicating that nonlinear heat radiation is present in the irregular flow of a non-linear Maxwell fluid with magnetohydrodynamic (MHD) boundary layer moving over a stretch surface. Calculation of heat and mass transmission is performed considering convective boundary conditions and chemical conversion of the first order. Several non-dimensional velocity, temperature, and concentration parameters are studied as a result of the developing parameters. There has been a recent study by Nuwairan *et al.*[28] on Darcy flow magnetohydrodynamics in non-Newtonian liquids. The Fourier law of

heat conduction generates the temperature distribution in the presence of a heat sink/source. A Soret-Dufour effect is also examined in mass concentration equations, which reveals that increasing the Deborah number causes the amount of radial and angular motion as well as the amount of axial flow to decrease. As a result of nanoparticle dispersion in the fluid, Brownian diffusion and thermophoretic diffusion can also be observed.

The work of Haritha *et al.* [29] examined an unsteady flow phenomenon Maxwell fluid in the presence of a magnetic field, thermal radiation, a source of heat, and chemical change in a context of Navier slip in combination with convective boundary conditions. Maxwell fluid boundary layer fluxes have lately attracted a lot of attention due to engineering applications. A continuous two-dimensional mixed convection stagnation point flow of nanofluids flowing through a vertical plate has been quantitatively investigated by Abdullah *et al.*[30] which is infected by the radiation, Dufour and Soret effects. As a result of stronger mixed convection, skin friction, mass transmission, and heat transmission rates will increase. The combination of heat transmission and mass transmission influences magnetohydrodynamic MHD natural convection in viscoelastic flows of fluid, as was explored by Riaz *et al.*[31]. A classical integral transformation technique (Laplace) is used to solve a set of equations that includes a dimensionless model equation and a modified boundary condition equation. The solutions are presented in closed form in this study. The resulting generalized results are especially important because they have a broad variety of implications in technology and applied sciences; a few of them are described here as limited examples. Graphical simulations are also utilized for parametric analysis of system parameters.

The features of (MHD) flow of Maxwell fluid across a flexible, spinning disc that convectively heated was investigated using a new mathematical model. A novel mathematical model is proposed to study the distribution of the heat transmitted from a convectively heated stretching and spinning disc as a function of its magnetohydrodynamic (MHD) Maxwell fluid flow characteristics. A basic isothermal system that covers both homogeneous and heterogeneous procedures is employed to govern the thermal transport of the fluid at the top layer. The effect of nonlinear thermal radiative heat flow on thermal transmission characteristics was studied by Khan *et al.* [32]. During homogeneous-heterogeneous reactions, the numbers of particles in the reaction mixture can be reduced as a result of magnetic flux, increasing temperature, and lowering velocity components.

Microorganisms, which are denser than water, typically swim upward, which causes bioconvection. Because of the growth of microorganisms, the suspensions' upper surface can become unstable and drop to the bottom, resulting in bioconvection. Swimming organisms are responsible for maintaining this bioconvection pattern by returning to the surface. Several researchers have investigated at how these bacteria affect the stability of bioconvection. There are several uses for bioconvection, including the pharma sector, polymer synthesized biologically, applications that protect the environment and are ecofriendly, technology for sustainable fuel cells, improve oil recovery by microbes, biosensors, biotechnology, and improvements in mathematical modeling. Innovative fractional derivatives have yet to be used to unsteady bioconvection in the literature. Their fractional models, which are unsolved issues in applied mathematics, can still be discussed both theoretically and experimentally. Typically, these situations are modeled using classic integer-order partial differential equations (PDEs).

During the process of bioconvection, random movements of microorganisms occur in shallow suspensions in which bottom heavy algae as well as oxytactic bacteria swim in different ways. In each of these examples, rational continuum models for low cell volume fraction have been developed and tested. These will be discussed, as well as recent theoretical and experimental discoveries, such as nonlinear pattern analysis, dispersing in shearing flow, studies of algal cell swimming behavior, and new attempts to construct a model for highly concentrated suspensions. Hill *et al.*[33] reviewed all work in this area from 1992 to 2005.

According to the work of Kuznetsov *et al.* [34] nanofluids containing gyrotactic bacteria are capable of initiating bioconvection. The critical Rayleigh number can be determined through the use of the Galerkin method, resulting in an analytical solution. It depends on whether nanoparticles are distributed in a top-heavy or bottom-heavy manner in conventional nanofluids as to whether they lower or increase the Rayleigh number. On the other hand, gyrotactic bacteria are known for destabilizing properties.

As a result of the synergistic effect created by the interaction between viscous drag and gravity, bioconvection is the development of path convective motions in mixtures of swimming microorganisms. Swimming is driven via a balance of physical torques induced by a balance of physical torques created by an imbalanced mass dispersion within the organism. Gyrotaxis allows organisms to swim towards places with the quickest downflow

when they are heavier in the back. There are instances when bioconvective instability can arise in the absence of unstable density stratification due to the presence of gyrotaxis in a suspension that is initially uniform. Pedley, [35] created a model focused on the analysis of the linear instabilities found in a homogeneous blend of gyrotactic microorganisms. This model aims to enhance our comprehension of suspensions comprising gyrotactic microorganisms. A suspension becomes unstable when its wave number falls below a specific threshold value, which is determined by calculating the wave number of the two most rapidly increasing disturbances. If the cell is sufficiently elongated, a convection pattern can be projected.

The development of high-density heat-generating systems requires efficient thermal transmission. The possibility of using nanofluid is important in this need. Mariam *et al.*[36] conducted a study exploring the impact of gyrotactic microbes on the flow of non-Newtonian fluid (Maxwell fluid) over a cylindrical surface that expands. Determining the Maxwell nanofluid's heat and mass transit is the major goal of this research. The zero-mass flow condition and the flow boundary condition are both considered as well. The boundary layer estimation is used in mathematical derivation. Zhang *et al.*[37] studied the flow of nano-fluids 3D in the context of a spinning circular surface loaded with nanoparticles and gyrotactic bacteria. To figure out the effect of torque on the plates at different magnetic field levels, a modified magnetic Reynolds number was applied. The study indicated that reducing the Reynolds number had a notable effect on temperature, microbe, and nanoparticle concentration profiles, which were found to be closely linked to conventional mathematical formulas. In order to test the novel bioconvection model proposed by Bees *et al.*[38] they examined the beginning of pattern development in a layer of limited depth. This is the first examination of bioconvection using a model that logically addresses microorganisms randomly swimming in a realistic geometry. The impacts of a swimming speed distribution, which have not previously been addressed in theoretical publications, have been considered. First pattern wavelength predictions are pretty close to the observed ones, but for a fair comparison, better experimental measurements of important factors are required.

According to the theory developed by Pedley, Hill, and Kessler (1988), a suspension of negatively buoyant microorganisms swimming in a suspension of positively buoyant microorganisms in a solution is affected by gyrotaxis and can maintain linear stability as the

suspension is shaken. Rayleigh numbers, Schmidt numbers, layer depth parameters, gyrotaxis numbers G , and geometrical parameters that characterize the ellipticity of microorganisms are the five dimensionless characteristics that define the suspension: the Rayleigh number, the Schmidt number, the layer-depth parameter, and the geometrical parameter that determines the microorganism's ellipticity. When the layer depth increases, the suspension becomes less stable, and the equilibrium does not occur. Over stable or oscillating modes occur when parameter levels are achievable experimentally. The exploration of how water-based nanoparticles with gyrotactic microbes move in a cylindrical shape has been conducted by Khan *et al.* [39] through the application of a mathematical model. They specifically studied the convection boundary-layer flows under a convective boundary condition. The numerical findings for nanoparticle concentration, motile microbe density profiles, and local motile microorganism density number are all obtained and examined. Upon investigation, it was determined that an increase in surface roughness resulted in enhancements in the movement of microorganisms, along with the Sherwood and Nusselt numbers, as well as skin friction.

Using gyrotactic microorganisms as a model, Saleem *et al.* [40] studied the effect of these gyrotactic microorganisms on nanofluid MHD flow. To try to explain the physical properties of the relevant parameters, graphs and numerical tables are employed as means of examining and debating the physical properties of the nanofluid and motile microorganism parameters used in the modeled nonlinear differential equations. With increasing bioconvection Peclet number, the rescaled density of motile microbes is observed to decrease, while with increasing Rayleigh number, the magnitude of the tangential velocity of motile bacteria is reduced and their low density is augmented.

Childress *et al.* [41] suggested a model for producing patterns while moving within layered suspensions of microorganisms that display negative geotaxis. A diffusion coefficient tensor D and an overall upward swimming speed U are used to characterize the organism's motility and it is also demonstrated that whenever the layers of depth or the overall species concentration exceeds a critical point, the equilibrium suspension is unstable to extremely small disturbances. The appropriate pattern size for deep layers is explicitly determined by the maximum growth rate in relation to U and D . Patterns produced by the ciliated protozoan *Tetrahymena pyriformis* are used for comparison with the results.

In the study of Kuznetsov *et al.* [42] a macroscopic convective motion which is produced by oxytactic microorganisms swimming upwards combined with mass flux produced by heat from below is referred to as thermal convection, a macroscopic convective motion created for a fluid coating by density stratification brought on by oxytactic microorganisms swimming upward. Geng *et al.* [43] aimed to investigate numerically how tiny solid particles can affect the formation of a bioconvection plume when microorganisms that are motile and gyrotactic move off-stream in the direction of the steady state plume. According to Aziz *et al.* [44] bioconvection parameters were studied in relation to their effects on the non-dimensional velocity, and concentration of nanoparticles, and motile microorganisms concentration, along with the Sherwood, Nusselt, and motile microbe populations within the region. These studies suggest a significant influence of these factors on heat, mass, and motility transport rates.

When the upper surface of a chamber containing *Bacillus subtilis* is left exposed, it leads to the formation of complex bioconvection patterns due to the activity of the bacteria. The upper surface of a suspension of *Bacillus subtilis* is exposed to the environment when it is placed in a chamber, producing complex bioconvection patterns. An initially uniform suspension will have a larger density at the top of an originally uniform suspension because cells are heavier than water, swimming upwards on average. Consequently, the concentration of a suspension is bound to be greater towards its uppermost layer in comparison to its lowermost. In the initial phase of pattern formation, these attributes are included in equations of conservation for oxygen and cell concentrations, and are calculated through employment of a finite element technique. In shallow chambers, there is no oscillatory instability, however, in deep chambers where the critical wave number is higher than zero, the instability must be oscillatory. Hillesdon *et al.* [45] conducted a study that analyzed the behavior of the critical Rayleigh number in suspension under different conditions. They also suggested a more accurate definition for this factor. There are a number of qualitative elements that correspond to experimental observations in the linear instability solution.

The bioconvection flow of nanoparticle-carrying fluid between two concentric cylinders has been studied by Zhang [46]. As an alternative to the Lorenz force, a study on the heat transport of microparticles by bioconvection was also conducted. It is believed that minuscule particles circulate within the gap of two cylinders that are positioned concentrically and have different radii. A constant velocity is maintained by the first cylinder, while the second cylinder rotates at a constant speed. Moreover, as part of the heat and mass gradient,

microparticles follow the principles of thermophoresis as well as Brownian motion as part of the heat and mass gradient. It has been suggested that gyro-tactic microorganisms, which are swimming in the nanofluid, form bio-convection in response to the density gradient.

The potential application of bioconvection in detecting the movement of tangent hyperbolic nanofluid over a swiftly moving substrate was explored by Khaled *et al.* [47]. According to their theory, the movement of the sheet triggers the flow. In order to properly analyze the situation, the team factored in the nonlinear thermal radiation properties and subsequently transformed the energy equation. The study utilized the continuum model for bioconvection in a suspension of swimming, gyrotactic microorganisms proposed by Pedley, Hill, and Kessler (1988), along with Ghorai's [48] continuum model to explore the durability and maintenance of a two-dimensional material flow in narrow, tall chambers that lack pressured side walls. The Navier-Stokes equation was combined with a conservation equation for microorganisms during system regulation.

When a stretched surface is covered with a magnetohydrodynamic Prandtl hybrid nanofluid, the heat transmission properties are impacted by both bioconvection and chemical reactions. Shah *et al.*[49] conducted a study that focused on the examination of heat transfer properties regarding Prandtl hybrid nanofluid with the presence of bioconvection and chemical reaction effects over a stretched surface. The study investigated hybrid nanofluid on stretched sheets and its tilted magnetohydrodynamic, thermal linear radiations, bio-convection, and chemical reaction processes. A mathematical model is presented by Yin *et al.*[50] examining the impacts of chemical reactions on magneto-Sisko fluid flow through a stretched cylindrical containing motile microorganisms. It is also included in this mathematical model that thermal conductivity varies and heat sources and sinks are not uniform.

An analysis was conducted by Wang *et al.* [51] on the flow of Prandtl nanofluid within a two-dimensional boundary layer subjected to an aligned magnetic field. The study focused on displaying the physical parameters of Nusselt numbers and skin friction coefficient. Iqbal *et al.*[52] also the properties of a stationary, two-dimensional nanofluid made up of gyrotactic bacteria and nanoparticles. Additionally, the study investigates the flow of a nanofluid that is struck obliquely at a stagnation point. Converting the challenging system of partial differential equations (PDEs) into ordinary differential system through appropriate transformations is

necessary, given the complexities and high degree of non-linearity these equations display.

In their research, Song *et al.* [53] explored the flow of nanofluid over a slim, vertical needle, which contains gyrotactic microorganisms. They also consider the existence of a magnetic field within the incompressible liquid. The nanofluid model takes into account the significant impacts of thermophoresis and Brownian motion. Zuhra *et al.* [54] conducted a study on the behavior of a type of nanofluid called second-grade nanofluid. This type of nanofluid was mixed with nanoparticles and gyrotactic microorganisms to investigate its flow patterns. The study also studied how magnetohydrodynamics (MHD) affects this type of nanofluid, and analyzed the boundary conditions using a nanofluid model. The study focused on the flow of this mixture in two dimensions. This investigation focused on gyrotactic microorganisms, which experience compensatory torques brought on by gravity and shear impacts. Gyrotaxis uses rotating motion to regulate the orientation of upswimming microorganisms.

A method to examine the behavior of geotactic, gyrotactic, and chemotactic microorganisms in a thick liquid was introduced through mathematical modeling by Hopkins *et al.* [55]. By integrating a particular set of microorganisms to a discrete collection, the Navier-Stokes equations for fluid mechanics are utilized. The microbes act like focal points for the gravitational force in the fluid dynamics, and this greatly affects the liquid flow. Aspects such as physical forces, etc. are also considered. Swimming speed and direction are influenced by various factors, such as vorticity, gravity. The remarkable thermal transportation capabilities of nanofluid make its study of great importance in various industrial and engineering applications, especially when considering the effects of bioconvection. Therefore, in his study, Khan [56] aimed to explore the bioconvective micropolar nanoliquid flow over a thin moving needle that contains gyrotactic microorganism. The method of homotopy (HAM) is used for required outcomes of the problem.

Ali *et al.* [57] conducted an investigation that explores the attributes of bioconvection and mixed convection situated in the stagnation area of a rotating sphere. This analysis concentrates on the conditions generated by the flow of tangent hyperbolic nanofluid. The researchers incorporated nano-sized particles due to their uncommon attributes, and added auto-motile and gyrotactic microorganisms to increase stability and eliminate sedimentation. In order to obtain a numerical solution, the study utilized Galerkin-based finite element

discretization, and closely monitored the impact of variables through computing procedures. The motion of the sphere rotating and the Casson fluid caused the fluid to move faster along the x-axis while it slowed down in the y-axis. Brownian motion and thermophoresis played important roles as higher values of these parameters led to an increase in the temperature of the nanofluid.

The bioconvection of a nanofluid that includes motile gyrotactic microorganisms was investigated by Rashad *et al.* [58]. The nanofluid will flow past a horizontal circular cylinder under convective boundary conditions. The finite-difference algorithm to compute nonlinear problems is examined through the outcomes computation. Mallikarjuna *et al.* [59] have explored the continuous mixing of a nanofluid that carries gyrotactic micro-organisms along a vertical cylinder. The team has employed passively controlled nanofluid models to approximate this intricate nano bioconvection flow issue, which exhibits a more accurate representation of physical realism compared to actively controlled nanofluid models that were commonly used in the past.

Biological, medical, and engineering phenomena heavily rely on microorganisms. Ishikawa [60] discussed biomechanical research on interactions between swimming microorganisms. He begins by outlining studies on two-body interactions, which are considered the simplest form of many-body interactions. It was confirmed that existing mathematical models effectively capture the interactions between two closely located swimming microorganisms. It was noted that some collective motions, like the coherent structures of bacterial suspensions, can be explained by fluid dynamics. The impact of cellular suspension micro-structure on macroscopic suspension properties will be discussed as a final point. Khan *et al.* [61] investigated the flow over a porous wedge, factoring in viscous dissipation and Joule heating. Their analysis also considered magneto-hydrodynamic effects, as well as the existence of gyrotactic microorganisms in a nanofluid-saturated wedge. They tackled the problem through the application of the passive control model.

Kim *et al.* [62] have conducted a theoretical analysis on the impact of the Soret effect and Dufour effect on convective instabilities in nanofluids. The Soret effect is the induction of mass diffusion through thermal gradient, while the Dufour effect is the induction of heat transfer through concentration gradient. Through the implementation of linear stability theory under one-fluid model, a novel characteristic dimensionless group has been derived. As the initial concentration of nanoparticles and the Soret-Dufour effects rise, the convective motion

in nanofluids initiates without difficulty in accordance with the results of the instability analysis conducted under the prescribed conditions.

2.2 Research Gap

Above comprehensive literature survey prove that until now viscoelastic Maxwell fluid flow in thin layer near to boundary around a horizontal rotating and stretching cylinder with heat transportation under Soret-Dufour effect is not studied. Moreover, study of bioconvection phenomenon in Maxwell fluid which is flowing in a swirl motion of elastic cylinder is also not investigated. Thus, the present thesis work is comprised to fill this gap in the literature of non-linear fluid dynamics.

2.3 Research Objectives

In the presence of the cylinder's torsional motion, the Maxwell fluids around it will be examined. Under the effect of the bioconvection phenomenon, the flow will be further modified. Main objectives of this research are:

- Modeling of flow, heat and bioconvection equations and transformation with similarity variables for numerical computation.
- Investigation of the flow mechanism of viscoelastic fluid which is caused by rotating cylinder against Lorentz force resistance.
- The thermal energy and solutal transportation mechanism in view of Soret-Dufour phenomenon.
- The process of bioconvection occurrence in flow of Maxwell fluid

CHAPTER 3

PRELIMINARIES

3.1 Basic Definitions

This chapter offers some standard definitions and laws to help you comprehend the analysis in the next chapters.

3.1.1 Fluids [64]

There are multiple fields of engineering, including mechanical and chemical, as well as biological and astrophysical systems, use fluid mechanics. A substance that is capable of undergoing deformation or flowing persistently under the influence of an external force, such as shear stress, can be identified as a fluid regardless of whether it is liquid, gas or any other material.

3.1.2 Fluid mechanics [64]

The study of fluids and the forces acting on them. There are two distinct branches of applied mechanics that deal with the properties and behavior of fluids.

3.1.3 Fluid statics [64]

The branch of fluid mechanics that describes the characteristics of fluids at rest.

3.1.4 Fluid Dynamic [64]

The discipline of fluid mechanics that examines the properties of fluid flow.

3.1.5 Viscosity [64]

Essentially, viscosity refers to the resistance of a fluid (liquid or gas) to changes in shape or movements of neighboring parts relative to each other. Due to the internal friction caused by its molecular structure, viscous fluids resist motion due to their resistance to deformation at a certain rate. This is the reason why their viscosity is a measure of resistance to deformation at a particular rate. As a result of its molecular structure, low viscosity fluids tend to flow more smoothly when they are in motion since they cause less friction.

$$\mu = \frac{\tau}{\frac{\partial u}{\partial y}}, \quad (3.1)$$

where μ is viscosity coefficient, τ is shear stress and $\frac{\partial u}{\partial y}$ represents the velocity gradient or rate of shear strain.

3.1.6 Non-Newtonian Fluids [64]

Non-Newtonian fluids are characterized by their inability to follow Newton's viscosity law. This means that the viscosity should remain constant no matter how much stress is applied. When non-Newtonian fluids are under pressure, their viscosity can change from liquid-like to solid-like. There are many types of viscoelastic non-Newtonian fluids, such as polymer solutions, thermoplastics, granular materials, resins, paints, gels, and biological fluids that can be studied.

3.1.7 Newtonian Fluids [64]

A Newtonian fluid is one that possesses the property of being in compliance with Newton's law of viscosity.

3.1.8 Newton's Law of Viscosity [64]

It shows that the shear-stress of a fluid is linearly and directly related to the velocity gradient. The viscosity or viscosity coefficient is used to describe the connection between the

shear-rate and the shear-stress of a fluid at a particular temperature and pressure. It is mathematically represented as

$$\tau = \mu \frac{du}{dy}. \quad (3.2)$$

3.1.9 Kinematic viscosity [64]

Kinematic viscosity ν is defined as the ratio of fluid's density to its viscosity fluid in dynamic state. Its formula is

$$\nu = \frac{\mu}{\rho}. \quad (3.3)$$

3.1.10 Pressure [64]

The relationship between the amount of force F and the surface area A is expressed as pressure. Mathematically expressed as,

$$P = \frac{F}{A}. \quad (3.4)$$

3.1.10 Maxwell Fluids [66]

A Maxwell material is the simplest basic model viscoelastic material. Viscoelasticity is the property of materials deformed in continuum mechanics in a manner that exhibits both the qualities of viscosity and elasticity. It exhibits viscous flow on the long timescale, but extra elastic resistance to rapid deformations. It is named for the model's creator, James Clerk Maxwell, who suggested it in 1867. It is also known as a Maxwell fluid.

3.1.11 Maxwell Model

James Clerk Maxwell (1867) invented the Maxwell model, because of the elasticity and viscosity effects; this model is known as viscoelastic fluid, first which is built by connecting a linear spring with a dashpot in series, as illustrated in Fig. 3.1



Figure 3.1: Maxwell Model

When the load is removed (unloaded), the linear spring strain recovers instantly, but the viscous part of the strain does not return. As a result, the Maxwell model cannot represent viscoelastic material recovery and can only represent elastic recovery. The Maxwell model is a straightforward mathematical method for describing the rheological characteristics of numerous materials. The Maxwell equation is highly helpful in thermodynamics because it provides a set of relationships that enable physicists to alter some unknown quantities that are challenging to quantify in the actual world. Therefore, these values must be replaced by others that can be measured. The electrical conductivity of nanofluids is estimated with the help of Maxwell model.

3.1.12 The Kelvin-Voigt model

Due to the parallel arrangement of the spring and dashpot, the Kelvin-Voigt model demonstrates the main creep phenomena since both the spring and dashpot cannot grow simultaneously. The Kelvin-Voigt model, as shown in Fig.2, has a parallel configuration of a linear spring and a dashpot. This model exhibits the major creep problem due to a parallel structure of the spring and dashpot. As a result, this model cannot depict steady-state creep or stress relaxation. The spring wouldn't be capable to return to its initial length instantly after being relieved of stress ($t > t_1$). Under external pressure, the dashpot will experience compressive creep due to the force exerted on it by the spring. All creep strain will be recovered after a specific amount of time. Viscoelastic materials display a phenomenon called 'viscoelastic contraction' which holds great significance for these materials.

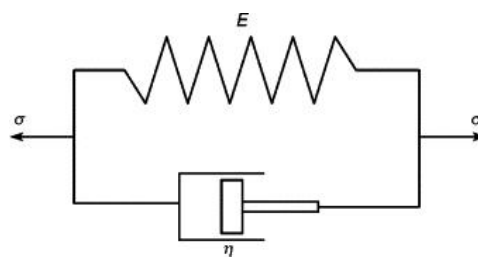


Figure 3.2: Kelvin-Voigt.

3.1.13 Zener Model

To explain the behaviour of viscoelastic materials, two types of models may be implemented. The Zener model, also known as the standard linear solid (SLS), is used to describe the elastic and viscous elements of a viscoelastic material using a linear arrangement of springs and dashpots. It is common for the Kelvin-Voigt and the Maxwell model to be used frequently in the calculation process. In the case of stress relaxation, however, these kinds models are frequently inadequate. For example, the Maxwell model does not address creep or recovery, and the Kelvin-Voigt model does not represent stress relaxation. SLS is the most basic model for predicting both phenomena. The SLS is significantly more complicated, including components in series as well as parallel.

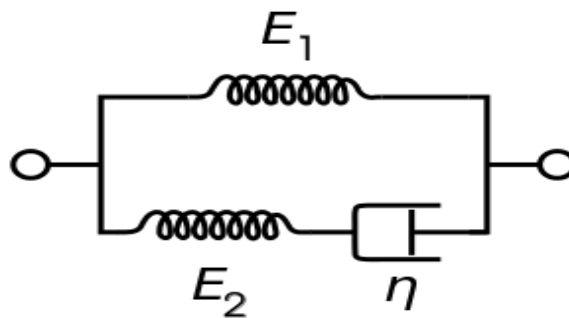


Figure 3.3: Standard Linear Solid (SLS) or Zener Model.

3.1.14 Swirling Flow

The tangential velocity of the fluid particles along an axis in a fluid flow, coupled with the axial velocity component produced by the tangential velocity, together produces the spiral or helical character of the flow. Swirling flow is used in many fluid machinery applications. Swirl phenomena have a major impact on devices such as combustion chambers, and cyclone separators.

Applications of Swirling Flow

Swirl flow plays a significant role in improving transmission of heat and many other technical

applications. In a very broad spectrum of industrial applications, swirling flows are utilized. Applications for non-reacting situations include whirlpools, tornadoes, heat exchangers, jet pumps, cyclone separators, and vortex amplifiers and reactors. The cyclone separator is a crucial application of limited whirling flow (hydro-cyclones for the separation of liquids). Two examples of whirling flow applications in chemical engineering are mixing by agitation and separation in cyclones.

3.1.15 Soret and Dufour Effect [66]

The Soret effect is the term used to describe the mass flow that is caused by a difference in temperature. The diffusion-thermo (Dufour) effect describes the energy flow produced by concentration changes. A temperature gradient induces a mass transfer process in mixes of two or more kinds of mobile nanoparticles, resulting in the Soret effect. As a result, it is often referred to as mass thermal diffusion. Thermophoresis is the transport force that happens when a temperature gradient exists. This force moves gas-borne particles with diameters smaller than 10 m towards the lower temperature region. Whereas the Dufour effect is the opposite of thermal diffusion. When two chemically distinct, non-reacting gases or liquids at the identical temperature are permitted to diffuse into one another, a temperature differential occurs within the system. The variation can reach several degrees in gases (for example, nitrogen with hydrogen), but it is measured in liquids.

Applications of Soret and Dufour effect

The Soret and Dufour effects are widely used in the geosciences and chemical engineering fields in real-life situations. It has been demonstrated by the Soret and Dufour effects that mass and heat are transported more efficiently when mixed with gases of extremely light and medium molecular weights. For example, the Soret effect has been utilized for separating isotopes. In the transfer of mass and heat on a flowing fluid, the Soret-Dufour factor is crucial. It is essential to the design of nuclear reactors, geothermal energy, groundwater pollution migration, oil reservoirs, isotope separation, production of rubber and plastic sheets, gas mixtures, compact heat insulation exchangers, and the disposal of nuclear waste, among other uses.

3.1.16 Lorentz Force [66]

When an electrically charged particle q moves with velocity v in both a magnetic and electric a force called the Lorentz force is generated. The force acts upon the charged particle in the direction it is moving while the magnetic field B acts in the opposite direction. The Lorentz force encompasses the entirety of the electromagnetic force F exerted on the charged particle. It is mathematically, expressed as

$$F = q(E + v \times B). \quad (3.4)$$

In order to divert electrons from travelling in a straight path and direct them to specific locations on the screen, a cathode ray tube television uses the Lorentz force theory. It is essential to many applications, including those involving electronic devices and motors, sensors, images, and biological ones.

3.1.17 Boundary Layer Theory [64]

A boundary layer is a thin covering of fluid formed when fluid flows across the surface of a bounding surface, creating a no-slip boundary condition. It is a thin covering of a flowing gas or liquid that comes into contact with an object, such as the interior of a pipe or an aeroplane's wing. The fluid in the boundary layer is subjected to shear forces, which cause it to flow laminar or turbulent depending on its velocity and viscosity.

3.1.18 Laminar Flow [64]

When a fluid flows within a pipe or tube, it can create laminar flow, which is characterized by parallel layers of fluid moving without any interference between them. Laminar flow is the motion of a fluid in which each particle follows the same path as the ones before it. Laminar flows are streamlined and smooth. Laminar flow is indicated by a small Reynolds number.

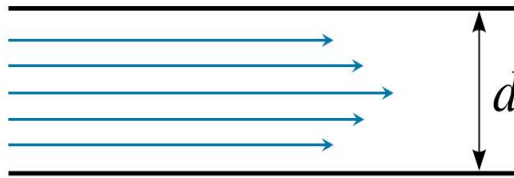


Figure 3.4: Laminar Flow

3.1.19 Turbulent Flow [64]

Fluids (liquids or gases) flowing unevenly or changing their composition describe turbulent flow. Turbulent flow is characterized by the uneven motion of fluid particles caused by the turbulent flow. The movement of fluid particles in a random direction is known as turbulent flow. In highly viscous fluids turbulent flow mostly occurs at very low velocities. The presence of turbulent flow is indicated by a high Reynolds number.

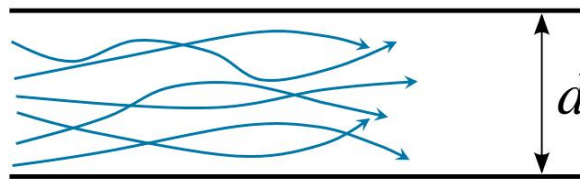


Figure 3.5: Turbulent Flow

3.1.20 Heat Transfer [64]

According to the First Law of Thermodynamics, heat transfer is the process of which molecules move from higher temperatures to lower temperatures. As the name implies, heat transfer occurs when molecules move from a high temperature area to a lower temperature area. As a result of heat transfer, the internal energy of both systems is changed in accordance with the First Law of Thermodynamics. Over the last several years, researchers and experts have paid close attention to the advancements achieved in the development of advanced heat transfer fluids.

3.1.21 Conduction [64]

Heat is transported from one item to another due to the collision of molecules in contact; this phenomenon is known as conduction. Such heat transmission takes place in solids. Transfer of heat from hot to cold end of an object is conduction. It is mathematically represented as

$$q = -k\nabla T, \quad (3.5)$$

where, q represents the density of local heat flow, $-k$ conductivity of a substance and ∇ is temperature gradient.

3.1.22 Radiation [64]

The transference of energy in the form of waves or particles over a space or a medium is known as radiation. It occurs in liquids and gases as well as the atmosphere.

3.1.23 Thermal Conductivity [64]

Thermal conductivity is a characteristic that specifies the capacity of a substance to conduct heat. Thermal conductivity defines how easily heat passes through a substance. Significant uses for thermal conductivity include steam generators, electrolytes, concrete heating, and laminating. Thermal conductivity is also defined as the energy transmission caused by the spontaneous movement of molecules across a temperature gradient.

3.1.24 Thermal Diffusivity [64]

Whenever a substance's thermal diffusivity is expressed as the ratio of its unstable heat conduction to its specific heat capacity, it is calculated as the product of the specific heat capacity C_p and ρ density. It is mathematically expressed as

$$\alpha = \frac{k}{\rho C_p}, \quad (3.6)$$

where, k is thermal conductivity, C_p is specific heat and ρ is density.

3.1.25 Mass Diffusivity [64]

Molecular diffusion is characterized by a proportionality constant between the molar flow and the gradient in the species' concentration as the result of molecular diffusion. This is called diffusivity, mass diffusivity, or diffusion coefficient (or the driving force for diffusion). Mathematically, expressed as

$$J = -D \frac{dC}{dx}, \quad (3.7)$$

where, D is diffusion coefficient, C is concentration, x is distance and J is flux.

3.1.26 Convection [64]

The physical movement of fluid (liquid, gas, or plasma) from one location to another to transmit thermal energy is known as heat convection. Heat convection is typically the dominant mechanism of energy transmission in liquids and gases. Convection, along with radiation and conduction, is one of the three major ways of heat transport. Natural (free) convection and forced convection are the two forms of heat convection. In most circumstances, both kinds coexist, which is referred to as mixed convection. Convection heat transfer is determined using a unit of conductance called the convective heat-transfer coefficient. Convection is a method of moving heat that is also known as a heat transfer process. Heat is transferred through mediums that flow, like water or air. During convection, temperature variations within a fluid result in convection. Convection can take two forms: natural convection and forced convection. Over a vertical flat surface, the free convection boundary layer has been a major research topic for a long time. It is likely the first buoyant convective problem to have been researched.

Natural Convection

In natural convection, or convection without the aid of external forces, the fluids move in a way that does not require any external forces in order to occur. A fire can cause hot air to expand while a difference in pressure can lead to the melting of ice, there may be a sea wind or land breeze and blood circulation of warm-blooded creatures.

Forced Convection

When fluids are pushed to circulate in order to improve heat transmission, this unique kind of heat transfer is known as forced convection. A ceiling fan, a pump, a suction tool, water heaters or geysers for quick water heating.

Mixed Convection

When heat is transported through a combination of natural and forced convection mechanisms, fluid thermodynamics refers to this phenomenon as mixed convection. This is sometimes described as circumstances in which buoyant forces and pressure forces interact. The term for the sort of heat transfer that comes from the interaction of free and forced motions in this situation is mixed convection flow.

Applications of Mixed Convection

In many technical, industrial, and natural settings, mixed convection flows which is usually defined as combined free- and forced convection flows occur. Forced convection is frequently utilized in applications such as fan-cooled electronic component cooling and forced air blower-heated house heating. Warm-blooded animals' blood circulation. Biotechnology, chemicals, ethanol, amino acid micro sensors, mixed convection, and a variety of ecosystems are just a few examples of applications for this process.

3.1.27 Bioconvection [65]

Numerous microorganisms live in practically every imaginable watery habitat on Earth and are believed to account for a significant portion (more than 50%) of the world's biomass. Most people live in the oceans since that are where the majority of the water resides. Many of these are phytoplankton, the light-converting bottom link of the food chain, but many other species exist in vast and tiny bodies of fresh water. Since 1848, bioconvection patterns have been studied, and numerous observations have been made. Bioconvection occurs as microorganisms, with a higher density compared to that of water, exhibit an upward swimming trend on average. Bio-convection refers to pattern-forming convection motions created in suspensions of swimming microorganisms. The cellular streaming trend was discovered in

liquid suspensions of floating microorganisms, where fluid flow patterns continue downwards in areas with high concentrations of microorganisms and swim upstream in areas with low concentrations. Bioconvection is the term used to describe pattern-forming convective movements that occur in suspensions containing swimming microorganisms. These movements are propelled by a combination of physical torques due to gravity and viscous drag, which act on a mass imbalance inside the organism known as gyrotaxis. As the upper surface of the suspensions grows too thick due to microbe buildup, it becomes unstable, and microorganisms descend to the bottom, resulting in bioconvection. The microorganisms swimming upward are responsible for sustaining this bioconvection formation. Bottom-heavy alga and some oxytactic bacteria are the two most common forms of up swimming microorganisms employed in bioconvection research. Although their bioconvection patterns are extremely similar, their orientation processes are not (Hill and Pedley, 2005). Because of their unbalanced mass distribution, bottom-heavy microorganisms float upward in still water. As a result of shear flow and gravity pushing on the cell, Pedley et al., 1988 found that when such microorganisms are in a flow field, they are influenced by a balance of torques. In an oxytactic bacterial bioconvection study, the upper level of suspension is open, allowing the cells to swim toward areas of downwelling fluid. This allows the oxytactic bacteria to swim towards the downwelling fluid. Throughout their development, these microbes utilize oxygen as fuel and navigate towards areas with higher concentrations of it.

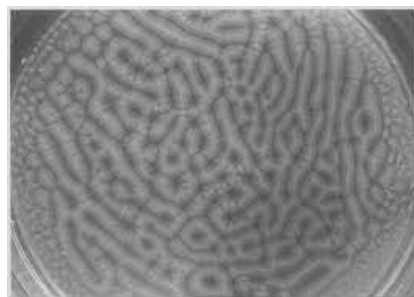


Figure 3.6: Pattern of Bioconvection.

Applications of Bioconvection

There are several uses for bioconvection, including the pharma sector, polymer synthesized biologically, applications that protect the environment and are ecofriendly, technology for sustainable fuel cells, improve oil recovery by microbes, biosensors, biotechnology, and improvements in mathematical modeling. In the subject of mechanics, bioconvection is also applied in a variety of ways, such as an energy source. Researchers have focused their attention in the last ten years on the motivating construction of the bioconvection phenomena in many engineering and industrial systems. Applications of bio-microbial systems, such as enzyme biotechnology, are used in the bioconvection phenomena. Understanding microorganisms and their environment with the use of systems biology is known as microbial systems. Enzymes are used in biotechnology to grow cultures and develop novel drugs. Enzymes are also used in food preservation. They provide services for cleaning and other environmental activities, as well as sickness diagnostics. Enzymes are now used in industrial biotechnology for a variety of objectives to produce new, sustainable goods quickly. Enzyme technology includes altering an enzyme's structure or catalytic activity to produce new metabolites or participate in novel reaction pathways.

Models of Bioconvection

Continuum Models

Continuous models assume variables are treated as continuous and ignore cell-cell contact. To achieve this, chamber length scales and concentration distributions are much wider than cell dimensions.

Microscale Models

Microorganisms are represented as individual organisms in a microscale model of bacterial swimming. This model represents highly complex geometries. Some examples include flagellar motion, hemodynamic interaction with moving bacteria, and bacterial absorption.

Particle Models

In 2002 Hopkins and Fauci presented a particle model of chemotaxis. They described microorganisms as discrete particles while ignoring the geometry (such as flagellar motion). They were able to do simulations with a huge number of particles by employing this simplified description of microorganisms.

3.2 Dimensionless Parameters

3.2.1 Reynolds numbers [65]

There is one dimensionless number known as the Reynolds number, and it can be used to determine whether a pipe has a laminar flow or a turbulent flow. It is regarded as one of the most important dimensionless numbers in the field of fluid flow. A fluid's Reynolds number is the ratio between inertial forces and viscous forces, which are both affected by relative internal movement as a result of varying fluid velocities. As a mathematical expression

$$Re = \frac{\rho u L}{\mu}, \quad (3.8)$$

where, ρ is fluid's density, u refers to flow rate, L refers to characteristic linear dimensions, and μ defining viscosity as a property of a fluid is dynamic.

3.2.2 Lewis Number [66]

It is derived from the ratio of heat diffusivity and mass diffusivity, and is dimensionless. The density of the concentration boundary layer is determined by comparing the thermal boundary layer thickness to the concentration boundary layer thickness with the help of Lewis number. And it is mathematically expressed as

$$Le = \frac{\alpha}{D}. \quad (3.9)$$

3.2.3 Prandtl Number [66]

It is a measure of momentum diffusivity, or in other words, how well momentum diffusivity is compared to heat diffusivity. The Prandtl number (Pr) is a dimensionless number. Mathematically, expressed as

$$Pr = \frac{\text{Momentum diffusivity}}{\text{Heat diffusivity}}$$

$$Pr = \frac{\nu}{\alpha}, \quad (3.10)$$

where, momentum diffusivity (kinetic diffusivity) is represented by μ and thermal diffusivity is represented by α .

3.2.4 Schmidt Number [66]

The Schmidt number (Sc) is a dimensionless measure that characterizes continuous fluid flow phenomena involving momentum and mass diffusion. It is calculated by dividing the kinematic viscosity, which represents momentum diffusivity, by the diffusivity. It is defined as

$$Sc = \frac{\nu}{D}, \quad (3.11)$$

where ν represents momentum diffusivity and D represents mass diffusivity.

3.2.5 Soret Number [65]

The Soret number is a non-dimension number, and it is ratio between the temperature difference to concentration. Mathematically, it is defined as

$$Sr = \frac{DK_T(C_W - C_\infty)}{\alpha_0 T_m (T_W - T_\infty)}. \quad (3.12)$$

3.2.6 Dufour Number [65]

It is the Dufour number (Du) that tells us how much the concentration difference contributes to the thermal energy flux due to the flow. Mathematically, expressed as

$$Du = \frac{Dk_T(C_W - C_\infty)}{\alpha_0 C_s C_p (T_W - T_\infty)}. \quad (3.13)$$

3.3 Conservation Laws

3.3.1 Mass Equation [64]

As fluids of constant density, mass must be maintained within a control volume under all fluid mechanics rules. Hence, the total mass that enters the control volume will be equivalent to the mass that departs from it added to the mass that accumulates within the control volume. This indicates that the mass that goes into the control volume must balance with the mass that goes out of it along with the mass that remains within it. Mathematically,

$$\left(\frac{\partial \rho}{\partial t}\right) + \nabla \cdot (\rho V) = 0. \quad (3.14)$$

3.3.2 Momentum Equation [64]

An equation of momentum which is a mathematical representation fluid flow phenomenon based on the momentum law, stating that the change in linear momentum of a volume moving with a fluid equals the force acting on the fluid from the surface and from the body. The total external forces that are applied to a fluid body are equivalent to the rate of change in momentum of the fluid body. It is mathematically, expressed as:

$$\rho \frac{dV}{dt} - \nabla \cdot \mathbf{S} - \rho \check{g} = 0. \quad (3.15)$$

In above equation, ρ is the fluid density, \mathbf{S} the extra stress tensor, $\tilde{\mathbf{g}}$ force of gravity.

3.3.3 Energy Equations [64]

The convection phenomenon is generally depend on the principle of conservation of energy, which mean it is essentially impossible to generate or destroy energy; the only thing that is possible is the transfer from one type of energy to another. The mathematical equation, which are use to describe the convection transport of both heat and solutal energy, stated as:

$$(\rho C_p) \frac{dT}{dt} = -\nabla \cdot \tilde{\mathbf{q}}, \quad (3.16)$$

$$\frac{dC}{dt} = -\nabla \cdot \tilde{\mathbf{j}}. \quad (3.17)$$

Where, $\tilde{\mathbf{j}}$ and $\tilde{\mathbf{q}}$ are define by well-know laws named as Fick's and Fourier's, respectively, specific heat-capacity of liquid with constant pressure is signified by C_p and (T, C) denote the fluid temperature and concentration distribution variables.

3.3.4 Fick's law

Fick's law states that the gradient of concentration proportionally affects the diffusion rate of a substance across a unit area.

3.3.5 Fourier's law

The flow of heat through an area perpendicular to the negative temperature gradient is directly proportional to the time rate of heat transfer.

3.3.6 Cell Conservation [34]

The microorganismic species movement in the fluid is express in the following relation: which deduce from cell conservation,

$$\frac{\partial n}{\partial t} = - \operatorname{div}(j), \quad (3.18)$$

$$j = n\mathbf{V} + n\mathbf{V}_0 - D_n \nabla n. \quad (3.19)$$

Here, j represents the flux of microorganisms, D_n represents the diffusivity of microorganisms species and \mathbf{V}_0 the average swimming velocity of cell.

CHAPTER 4

Flow of Maxwell Fluid engender by Swirling Motion of Cylinder

4.1 Introduction

As a result of a transverse magnetic field influencing a horizontal stretchable spinning cylinder, the Maxwell fluid flow with in boundary layer is examined in this chapter. In order to simplify partial differential equations (PDEs) that govern Maxwell fluid's twisting motion and energy transfer, the boundary layer concept has been proposed. The heat and mass transport characteristics of boundary layer flow across a stretched and rotating cylinder are also presented in this work. The numerically computed results are justified physically in the graphical abstracts form. Its significance and applicability in several domains of engineering and technology are addressed. Various researchers have carried out inquiries into the heat transfers and physical phenomenon occurring across an extended surface. It has various major industrial uses, including the plastic sheets extrusion, the condensation of metallic plates, and the manufacturing of glass filers. In this study, the impact of physical parameters is vied in graphical results.

4.2 Mathematical formulation

Consider a heated cylinder of radius R_1 immersed in a viscoelastic fluid under the impact of magnetic field being subjected to the swirling motion. Assume the flow velocity field is $\mathbf{V} = [u(z, r), v(z, r), w(z, r)]$, where along the (z, r) axes, respectively, and $\mathbf{B} = [0, 0, B_0]$ is the magnetic applied field across the r -axis. Let us assume that the cylinder rotates uniformly around its central axis and the rate at which it extends is directly related to its distance along the axial axis. Moreover, T_w and C_w are the assumed temperatures and

concentrations at the cylinder's surface. Figure 4.1 depicts the flow diagram.

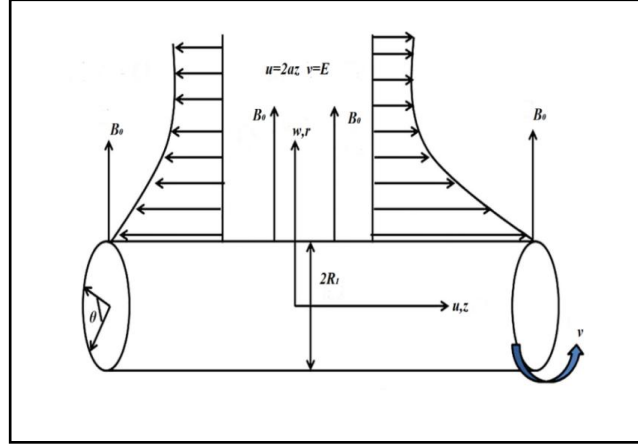


Figure 4.1: Flow Diagram.

In order to model this physical problem mathematically, the following governing equations (PDEs) are formulated in view of Eqs. (3.14 – 3.17) with addition of rheological relation of Maxwell fluid as:

$$\left(1 + \lambda_1 \frac{D}{Dt}\right) \mathbf{S} = \mu \mathbf{A}_1, \quad (4.1)$$

where λ_1 is the relaxation time, $\frac{D}{Dt}$ represents the Oldroyd derivative, $\mathbf{A}_1 = \nabla \mathbf{V} + (\nabla \mathbf{V})^T$ the first Rivlin-Ericksen tensor and μ the viscosity of the fluid. If $\lambda_1 = 0$, then Newtonian fluid condition can also be recovered.

$$\frac{\partial u}{\partial z} + \frac{w}{r} + \frac{\partial w}{\partial r} = 0, \quad (4.2)$$

$$u \frac{\partial u}{\partial z} + w \frac{\partial u}{\partial r} + \lambda_1 \left[u^2 \frac{\partial^2 u}{\partial z^2} + 2uw \frac{\partial^2 u}{\partial r \partial z} + w^2 \frac{\partial^2 u}{\partial r^2} \right] = -\frac{1}{\rho} \frac{\partial p}{\partial z} + v \left[\frac{\partial^2 u}{\partial r^2} + \frac{1}{r} \frac{\partial u}{\partial r} \right] - \frac{\sigma B_0^2}{\rho} \left(u + \lambda_1 w \frac{\partial u}{\partial r} \right), \quad (4.3)$$

$$u \frac{\partial u}{\partial z} + w \frac{\partial u}{\partial r} + \frac{wv}{r} + \lambda_1 \left(u^2 \frac{\partial^2 u}{\partial z^2} + 2uw \frac{\partial^2 u}{\partial r \partial z} + w^2 \frac{\partial^2 u}{\partial r^2} + \frac{2wv}{r} \frac{\partial w}{\partial r} + \frac{2uv}{r} \frac{\partial w}{\partial z} - \frac{2w^2 v}{r^2} \right) = v \left(\frac{\partial^2 v}{\partial r^2} - \frac{v}{r^2} + \frac{1}{r} \frac{\partial u}{\partial r} \right) - \frac{\sigma B_0^2}{\rho} \left(v + \lambda_1 w \frac{\partial v}{\partial r} - \lambda_1 \frac{wv}{r} \right), \quad (4.4)$$

$$u \frac{\partial T}{\partial z} + w \frac{\partial T}{\partial r} = \alpha_1 \frac{1}{r} \frac{\partial}{\partial r} \left(r \frac{\partial T}{\partial r} \right), \quad (4.5)$$

$$u \frac{\partial C}{\partial z} + w \frac{\partial C}{\partial r} = D_B \frac{1}{r} \frac{\partial}{\partial r} \left(r \frac{\partial C}{\partial r} \right), \quad (4.6)$$

The boundary conditions that apply to this flow situation, including the following:

$$\left. \begin{aligned} u(r, z) = 2az, v(r, z) = E, w(r, z) = 0, T = T_W, C = C_W \text{ at } r = R_1 \\ u = 0, T = T_\infty, C = C_\infty \text{ as } r \rightarrow \infty. \end{aligned} \right\} \quad (4.7)$$

Where $u, v,$ and w represent velocity components, T_W and C_W represent temperature and concentration at surface of cylinders. T_∞ and C_∞ represent temperature and concentration in the free stream.

The kinematic viscosity is represented by ν , thermal and mass diffusivity are represented by (α_1, D_B) , respectively. $a > 0$ denotes the strength of the cylinder's stretching with dimension T^{-1} , while E denotes the cylinder's constant torsion and has the same dimensions as velocity. By implementing the transformations group detailed below, it is possible to simplify the governing equations into ordinary differential equations.

$$\left. \begin{aligned} u = 2azf'(\eta), v = Eg(\eta), w = -aR_1 \frac{f(\eta)}{\eta^2}, \\ \theta(\eta) = \frac{T - T_\infty}{T_W - T_\infty}, \phi(\eta) = \frac{C - C_\infty}{C_W - C_\infty}, \eta = \frac{r^2}{R_1^2}, \end{aligned} \right\} \quad (4.8)$$

$$\eta f'''' + f'' + Reff'' - Ref'^2 - \beta_1 Re \left(\frac{f^2 f''}{\eta} + 2f^2 f''' + 4ff'f'' \right) - MRe \left(\frac{f'}{2} - \beta_1 ff'' \right) = 0, \quad (4.9)$$

$$\begin{aligned} 2\eta^2 g'' + 2\eta g' - \frac{g}{2} + 2Ren\eta fg' + Refg - \beta_1 Re \left(2f^2 g' + 4\eta f^2 g'' - 4ff'g - \frac{4f^2 g}{\eta} \right) \\ - MRe \left(g - 2\beta_1 fg' - \beta_1 \frac{fg}{\eta} \right) = 0, \end{aligned} \quad (4.10)$$

$$\eta\theta'' + \theta' + RePrf\theta' = 0, \quad (4.11)$$

$$\eta\phi'' + \phi' + RePrLe\phi = 0, \quad (4.12)$$

with transformed boundary conditions

$$\left. \begin{aligned} f(1) = 0, \quad f'(1) = 1, \quad g(1) = 1, \quad \theta(1) = 1, \quad \phi(1) = 1, \\ f'(\infty) = 0, \quad g(\infty) = 0, \quad \theta(\infty) = 0, \quad \phi(\infty) = 0. \end{aligned} \right\} \quad (4.13)$$

Above equations includes the dimensionless variables which are listed and defined as:

$\beta = (\lambda_1 a)$ is the Maxwell number, $Re = \left(\frac{aR_1^2}{2\nu}\right)$ represents the Reynolds number, $M = \left(\frac{\sigma B_0^2}{\rho a}\right)$, represents the magnetic parameter, $Pr = \left(\frac{\nu}{\alpha_1}\right)$ the Prandtl number and, $Le = \left(\frac{\alpha_1}{D_B}\right)$ is the Lewis number. Thus, following the Fang [5] to make convergence fast the variable η transformed as e^x .

$$f_{xxx} - 2f_{xx} + f_x - Re(f_x^2 - ff_{xx} + ff_x) - \beta_1 Re e^{-x}(2f^2 f_{xxx} - 5f^2 f_{xx} + 3f^2 f_x - 4ff_x^2) - MRe \left(e^x \frac{f_x}{2} - \beta_1 ff_{xx} + \beta_1 ff_x \right) = 0, \quad (4.14)$$

$$2g_{xx} - \frac{g}{2} + Re(2fg_x + fg) - \beta_1 Re e^{-x}(6f^2 g_x + 4f^2 g_{xx} + 4ff_x g - 4f^2 g) - MRe (g - 2\beta_1 e^{-x} fg_x - \beta_1 e^{-x} fg) = 0, \quad (4.15)$$

$$\theta_{xx} + RePrf\theta_x = 0, \quad (4.16)$$

$$\phi_{xx} + RePrL\phi_x = 0, \quad (4.17)$$

Boundary Conditions

$$\left. \begin{aligned} f(0) = 0, \quad f_x(0) = 1, \quad g(0) = 1, \quad \theta(0) = 1, \quad \phi(0) = 1, \\ \lim_{x \rightarrow \infty} e^{-x} f_x = 0, \quad g(\infty) = 0, \quad \theta(\infty) = 0, \quad \phi(\infty) = 0. \end{aligned} \right\} \quad (4.18)$$

4.3 Numerical Solution

In order to simplify the underlying PDEs that control the flow that occurs as a result of rotating and stretching cylinders with energy transport processes, the boundary layer theory is applied. The governing ODEs for flow and energy transportation are solved using the MATLAB numerical technique known as `bvp4c`. This function mainly based on extrapolation technique. For the implementation of this function 1st order ODEs require thus, for this aim the following variables are assumed:

$$f = y_1, \quad f_x = y_2, \quad f_{xx} = y_3, \quad f_{xxx} = yy_1, \quad (4.19)$$

$$g = y_4, \quad g_x = y_5, \quad g_{xx} = yy_2, \quad (4.20)$$

$$\theta = y_6, \quad \theta_x = y_7, \quad \theta_{xx} = yy_3, \quad (4.21)$$

$$\phi = y_8, \quad \phi_x = y_9, \quad \phi_{xx} = yy_4, \quad (4.22)$$

Resulting first order ODEs are:

$$yy_1 = \frac{2y_3 - y_2 + Re(y_2^2 - y_1y_3 + y_1y_2) + \beta_1 Re e^{-x}(3y_1^2y_2 - 5y_1^2y_3 - 4y_1y_2^2) + MRe\left(\frac{e^xy_2}{2} - \beta_1y_1y_3 + \beta_1y_1y_2\right)}{a_1}, \quad (4.23)$$

$$yy_2 = \frac{\frac{y_4}{2} - 2Rey_1y_5 + Rey_1y_4 + \beta_1 Re e^{-x}(6y_1^2y_5 - 4y_1y_2y_4 - 4y_1^2y_4) + MRe(y_4 - 2\beta_1 e^{-x}y_1y_5 + \beta_1 e^{-x}y_1y_4)}{a_2}, \quad (4.24)$$

$$yy_3 = -Re Pr y_1y_7, \quad (4.25)$$

$$yy_4 = -Re Le Pr y_1y_9, \quad (4.26)$$

where

$$a_1 = 1 - 2\beta_1 Re e^{-x}y_1^2 \quad \text{and} \quad a_2 = 2 - 4\beta_1 Re e^{-x}y_1^2 \quad (4.27)$$

With the above first order differential system, the associated BCs are

$$y_1(0) = 0, \quad y_2(0) = 1, \quad y_4(0) = 1, \quad y_6(0) = 1, \quad y_8(0) = 1, \quad (4.28)$$

$$\lim_{x \rightarrow \infty} e^{-x} y_2 = 0, \quad y_4(\infty) = 0, \quad y_6(\infty) = 0, \quad y_8(\infty) = 1. \quad (4.29)$$

4.4 Presentation of results

This section of the research work is established for an explanation of how the graphical results of the flow velocity, the thermal energy transport, and the total energy transport can be interpreted physically. By comparing Newtonian and non-Newtonian fluids with $Re = 2$ and $Re = 5$, it has been visually demonstrated that important parameters have a significant impact on velocity, temperature, and concentration fields. These parameters have stable values assumed to be $\beta_1 = 0.5$ for $M = 1$, for $Pr = 4.5$, and for $Le = 6.5$. For high values of Reynolds number, it is discovered that the fluid's velocity soon decays to free stream, resulting in the flow only occurring close to the cylinder's surface. Furthermore, non-Newtonian fluids with low Reynolds numbers is increased heat and mass transmission. Here, it is important to remember that the swirl velocity remains unaffected by the axial velocity when it is $Re = 0$.

Physically, the stretching of the cylinder decreases for zero Reynolds numbers, and the flow around the cylinder is caused entirely by the rotation of the cylinder in an axial direction. Moreover, the swirling motion of a cylinder fails to produce any axial flow of fluid due to its swirling nature. Reynolds number Re , Maxwell parameter β_1 , and magnetic parameter M are shown in Figures 4.2 (a – d) which suggest that the axial velocity field when these parameters are increased. According to the findings of the study, axial velocity decreases and decays exponentially as the three factors increase. It is clear from the plots in Figures 4.3 (a, b) that the swirl velocity decreases as Re and M increase. The outcome remains consistent for radial velocity, as illustrated in Figures 4.4 (a – d). When fluid flows and a transverse magnetic field is present, the Lorentz force is stronger with a higher magnetic parameter M value. This force acts as a counter to the velocity of the flow. This results in a reduction in fluid velocity. Viscoelastic fluids undergo stress relaxation phenomena when the Maxwell parameter β_1 is increased, resulting in the liquid becoming more solid-like, and thus resulting in a decrease in

fluid velocity as a result. There is a governing factor within Maxwell fluid flow called the Reynolds number. This ratio of surface stretching inertial force to viscous force is what is referred to as Re . This means that if Re is increased, the inertial force of the system will increase, thereby resisting the acceleration of the fluid. As an outcome, the flow field is reduced as a result of this point. It is physically observed that when the magnetic parameter M increases, the Lorentz force increases, which increases the efficiency of the transfer of energy between fluid particles. In addition, when greater values of the magnetic parameter M are used to compare Newtonian fluids with non-Newtonian fluids, the velocity of the fluid flow is increased and the transmission of energy is reduced, whereas the opposite tendency is observed for non-Newtonian fluids

It is obvious from the graphs of Figures 4.5($a - c$) and 4.6($a - c$) that the provided swirling flow mechanism transmits both thermal and solutal energy. There has been a finding that Reynolds number Re has a diminished impact both on temperature profile. A fluid flow field can be reduced by the Reynolds number in physical terms, which means that higher Reynolds numbers limit the principle convective mechanism that transfers energy by reducing the flow field. As a consequence, the temperature field decreases. A graphical representation of the solutal field reveals that increasing Maxwell's parameter significantly enhances the rate at which heat and mass are transferred in a flow by increasing the value. It is well known that, as the value of β_1 increases, the fluid behavior becomes more solid-like, and as a result, the transmission of thermal. Here is also a comparison between the Prandtl number Pr and the Lewis number Le to determine how thermal and solute energy transit in fluids relates to momentum transport, respectively. The temperature and concentration fields of fluid are affected when the dimensionless numbers Pr and Le increase. This happens because the fluid's thermal and mass diffusivity decrease as a consequence of higher Pr and Le values. This graphical representation of axial and swirl velocity fields is illustrated in Figures 4.7 (a, b) and 4.8 (a, b) as the Maxwell parameter β_1 and magnetic parameter M increase in flow analysis for extremely large Reynolds numbers Re , resulting in a decrease in axial and swirl flow velocity. These results indicate a decrease in both axial and swirl flow velocities. It is important to note that the physical rationale for this drop in axial and swirl velocities is exactly the same as it is for larger values of β_1 and M .

As a result of the graphical results shown in Figures. 4.9 (a, b), and 4.10(a, b), it can be observed that the physical process of energy transmission in the whirling flow of Maxwell fluid with extremely large Reynolds numbers can be examined. It can be seen that as the values of η and M increase, so does the transmission of heat and solute energy. The flow of thermal and solute energy becomes increasingly intense. The transmission of energy in fluid particles experiences an increase as the Lorentz force rises due to an increase in the magnetic parameter M , in terms of the physical aspect. In this scenario, we see the same tendencies as in Case B because the Lorentz force increases. Moreover, when greater values of the magnetic parameter M are used to examine Newtonian and non-Newtonian fluids, it is observed that Newtonian fluids have a faster fluid velocity distribution, as well as fewer energy transmissions, whereas the reverse tendency is observed for non-Newtonian fluids.

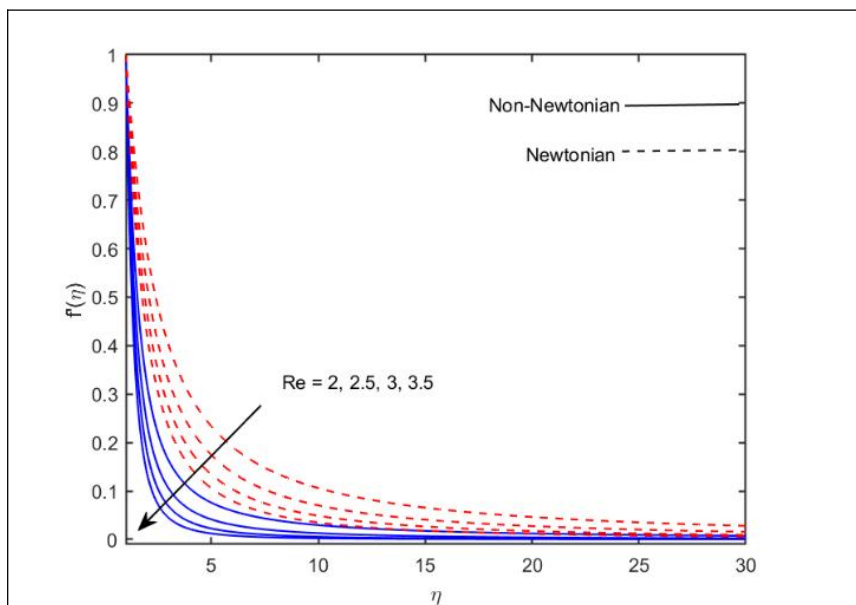


Figure 4.2 (a): Variation in $f'(\eta)$ for increasing values of Re .

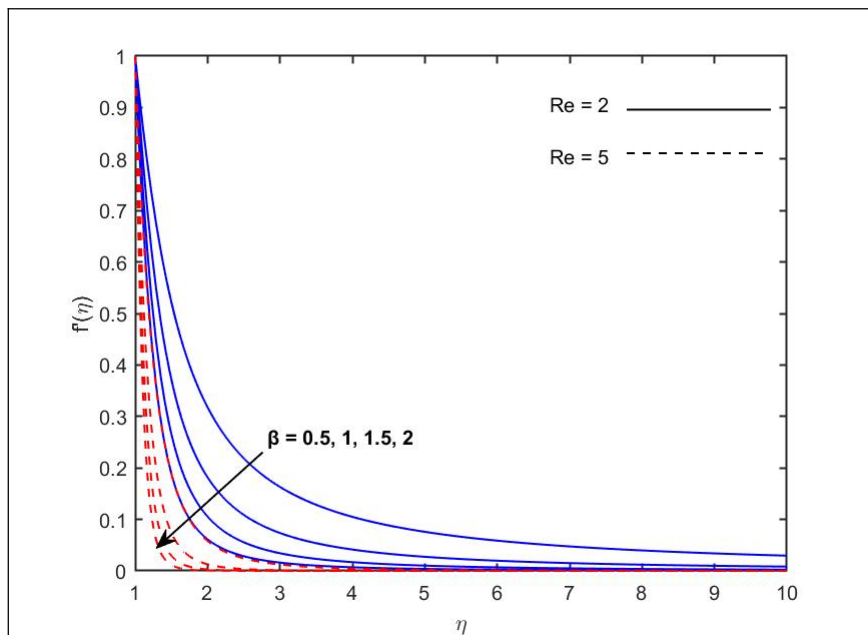


Figure 4.2 (b): Variation in $f'(\eta)$ for increasing values of β_1 .

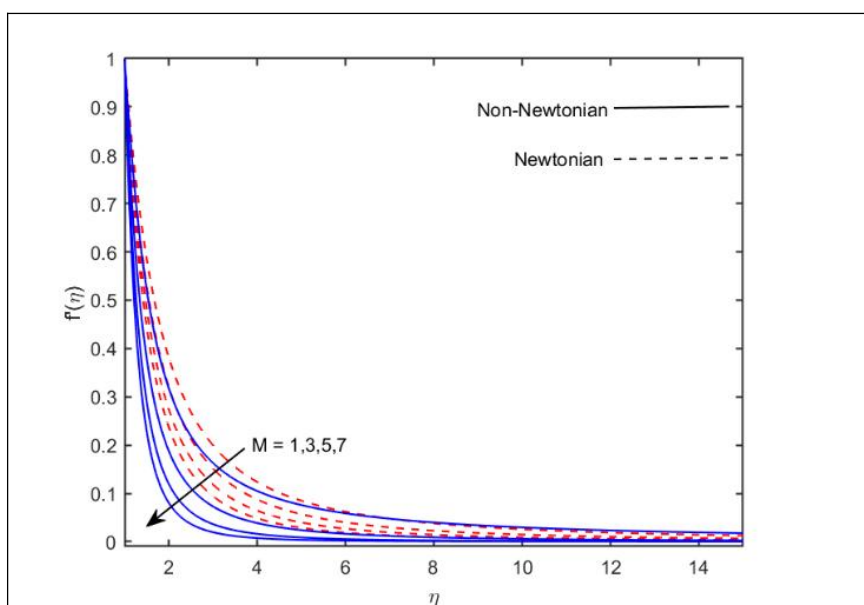


Figure 4.2 (c): Variation in $f'(\eta)$ for increasing values of M .

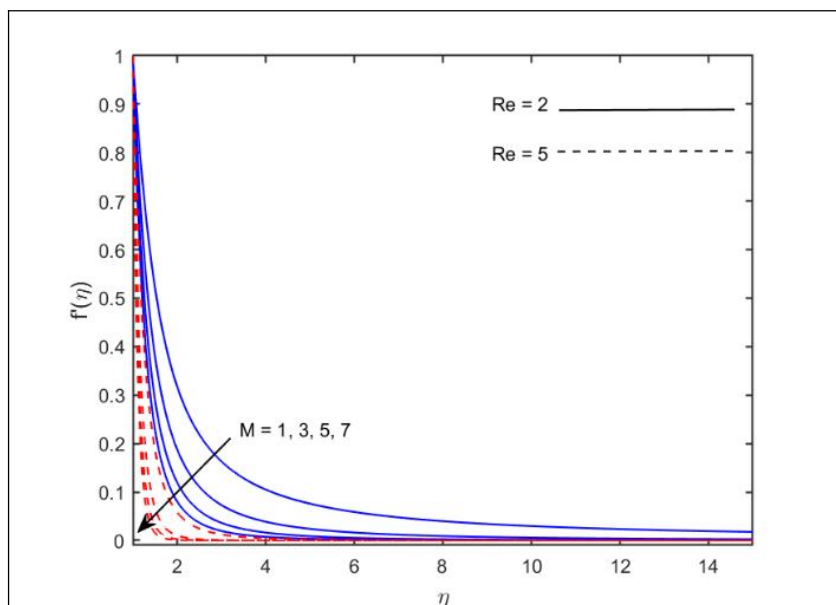


Figure 4.2 (d): Variation in $f'(\eta)$ for higher values of M .

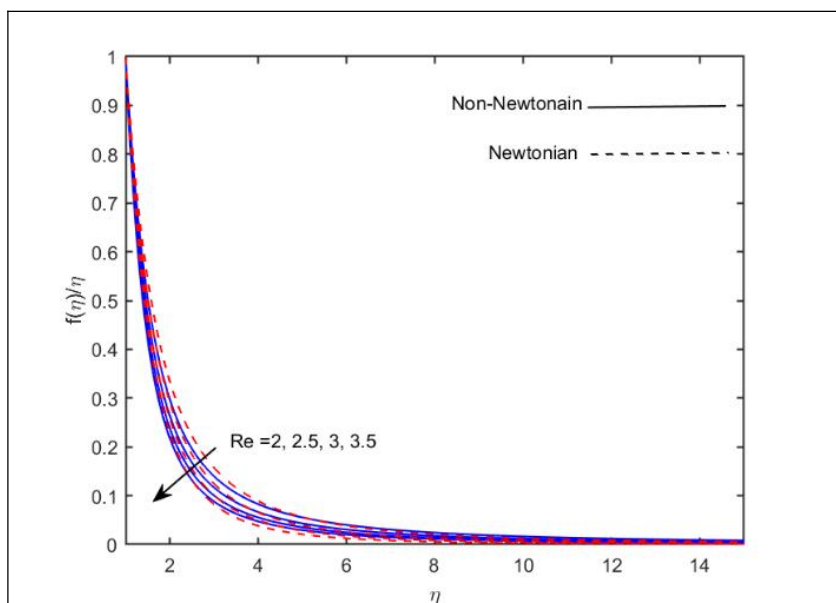


Figure 4.3 (a): Variation in $f(\eta)/\eta$ for various values of Re .

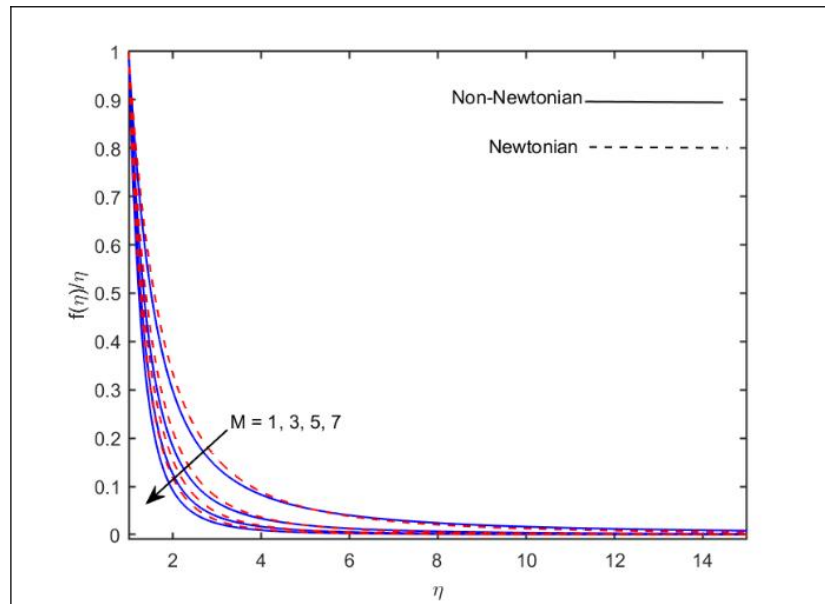


Figure 4.3 (b): Variation in $f(\eta)/\eta$ for various values of M .

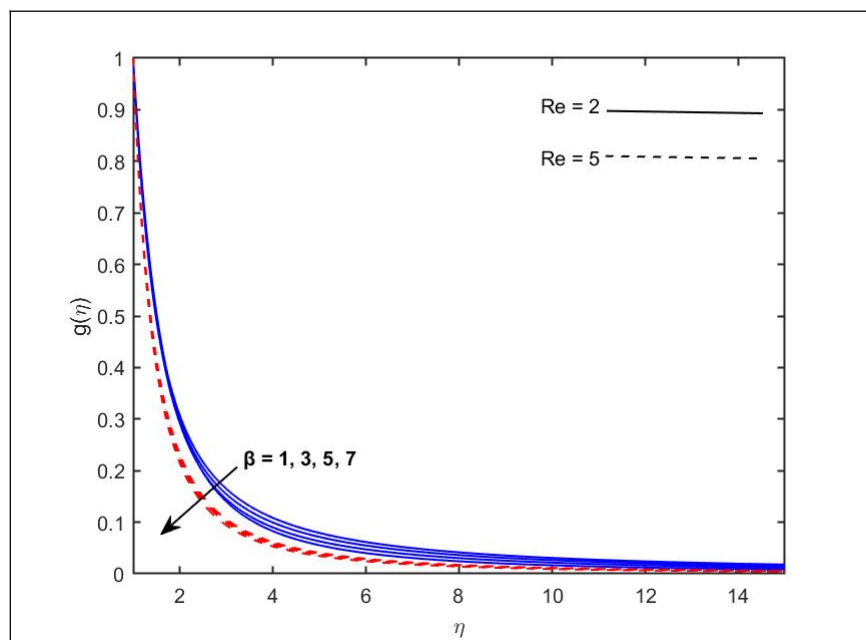


Figure 4.4 (a): Change in $g(\eta)$ for increasing values of β_1

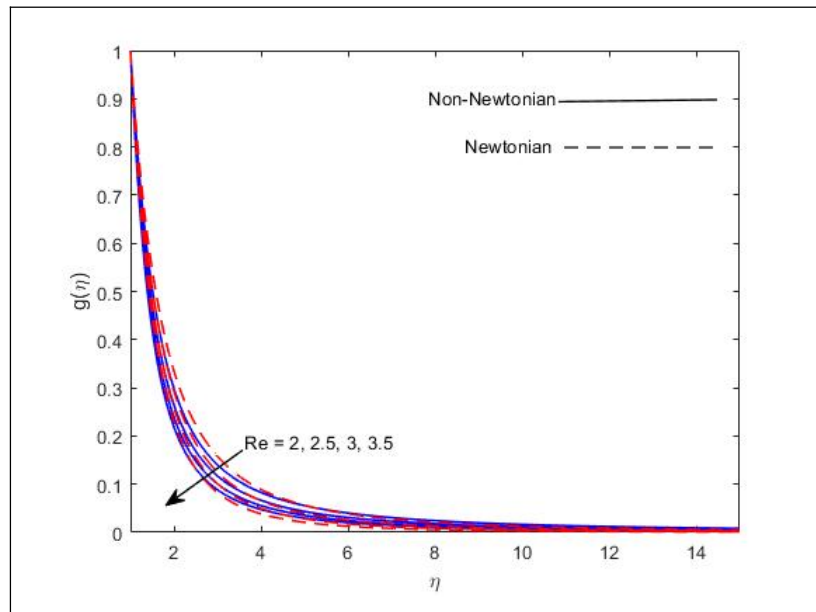


Figure 4.4 (b): Change in $g(\eta)$ for increasing values of Re

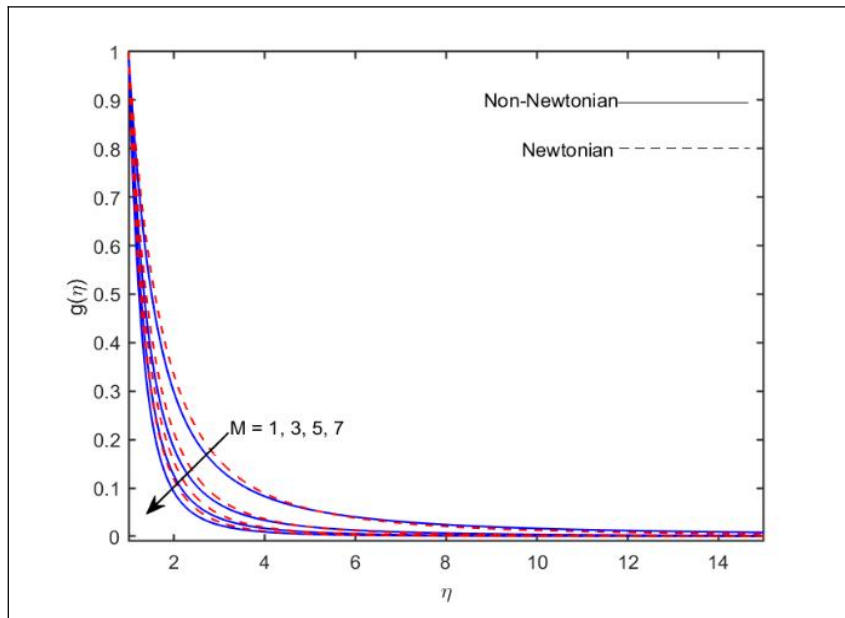


Figure 4.4 (c): Trend of $g(\eta)$ for higher values of M .

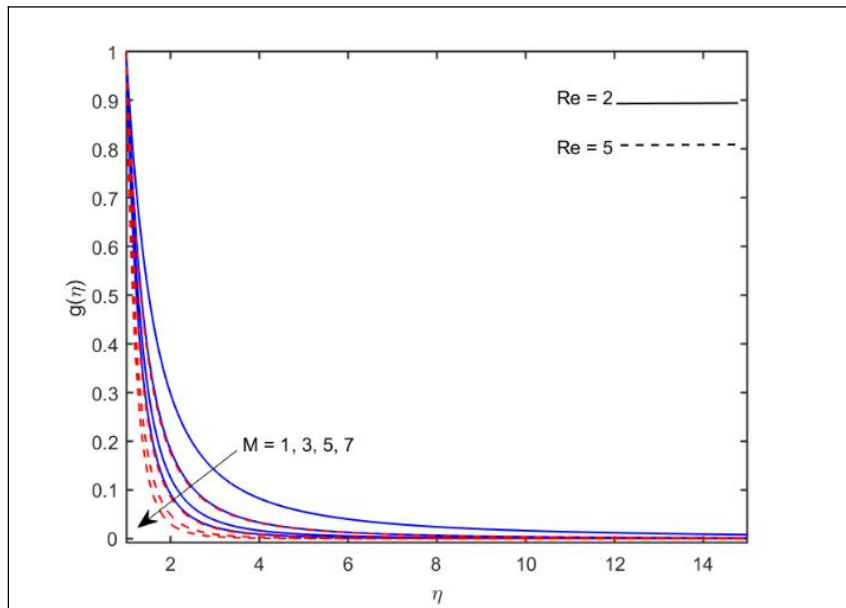


Figure 4.4 (d): Change in $g(\eta)$ for increasing values of M .

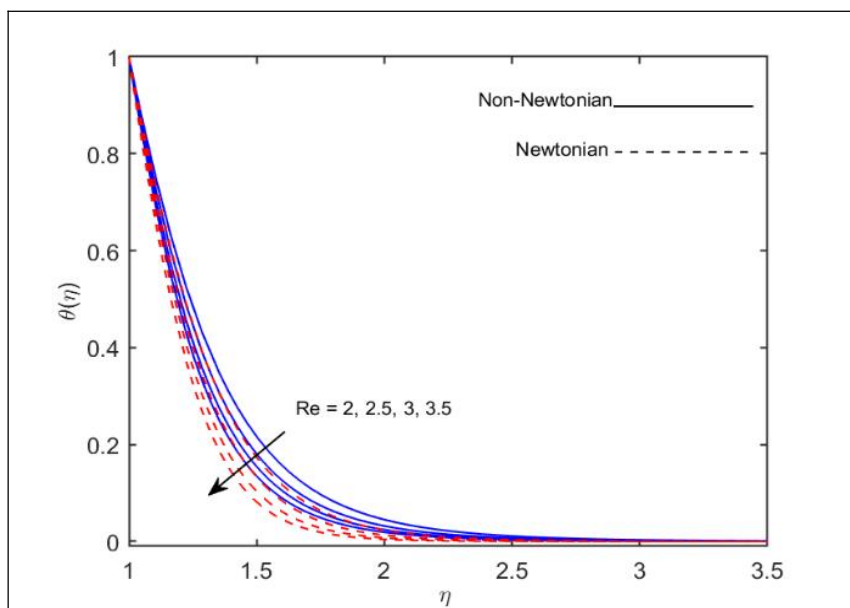


Figure 4.5 (a): Change in $\theta(\eta)$ for increasing values of Re .

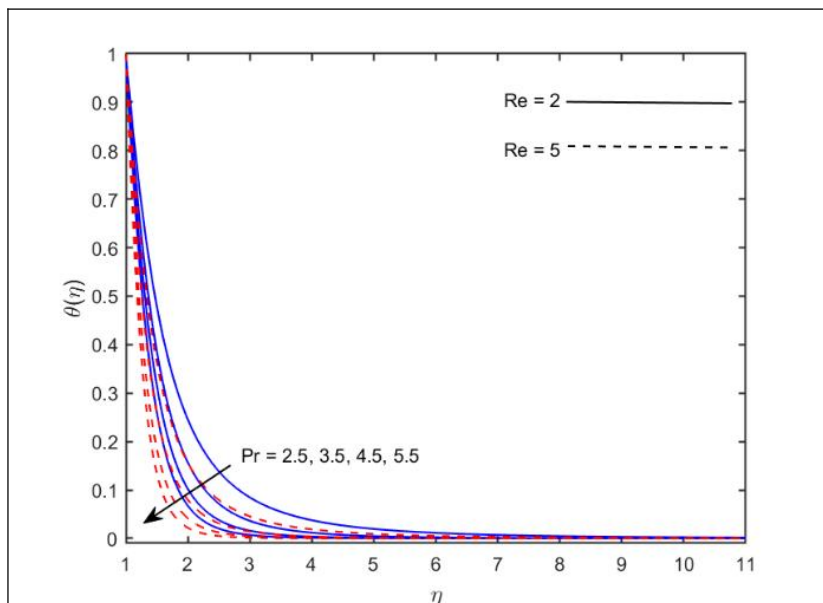


Figure 4.5 (b): Change in $\theta(\eta)$ for increasing values of Pr .

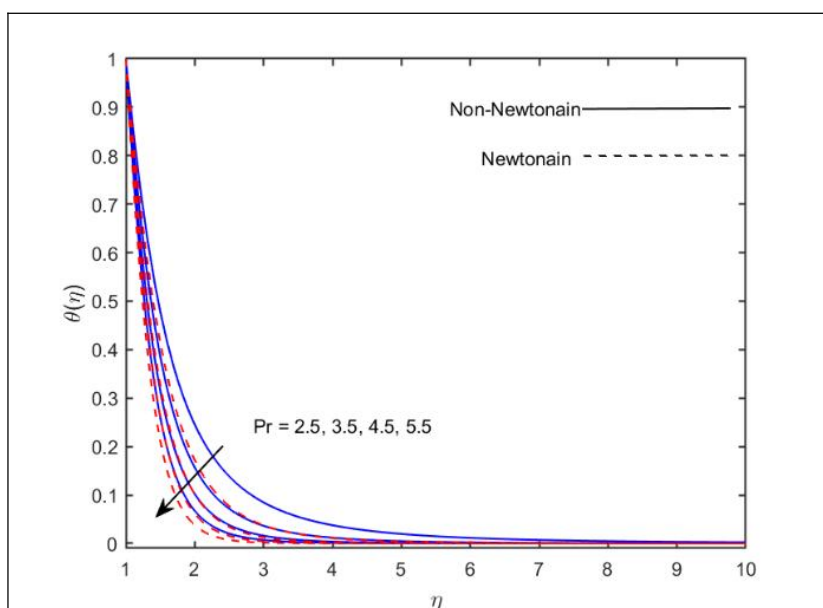


Figure 4.5 (c): Change in $\theta(\eta)$ for increasing values of Pr .

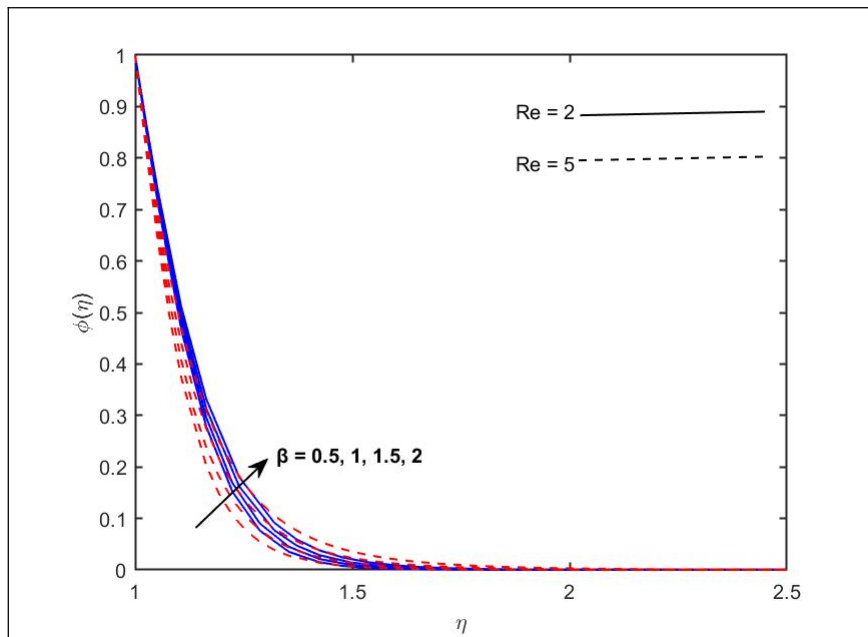


Figure 4.6 (a): Change in $\phi(\eta)$ for increasing values of β_1 .

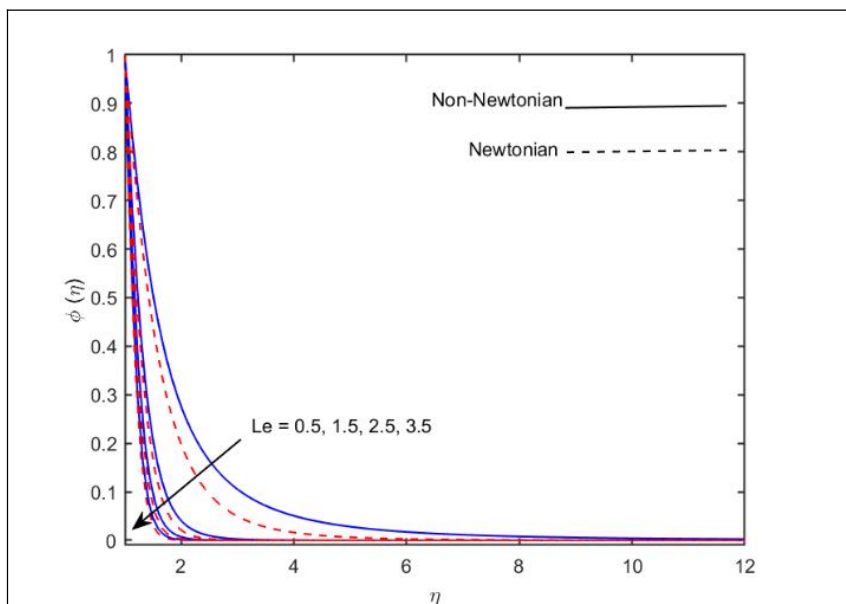


Figure 4.6 (b): Change in $\phi(\eta)$ for increasing values of Le .

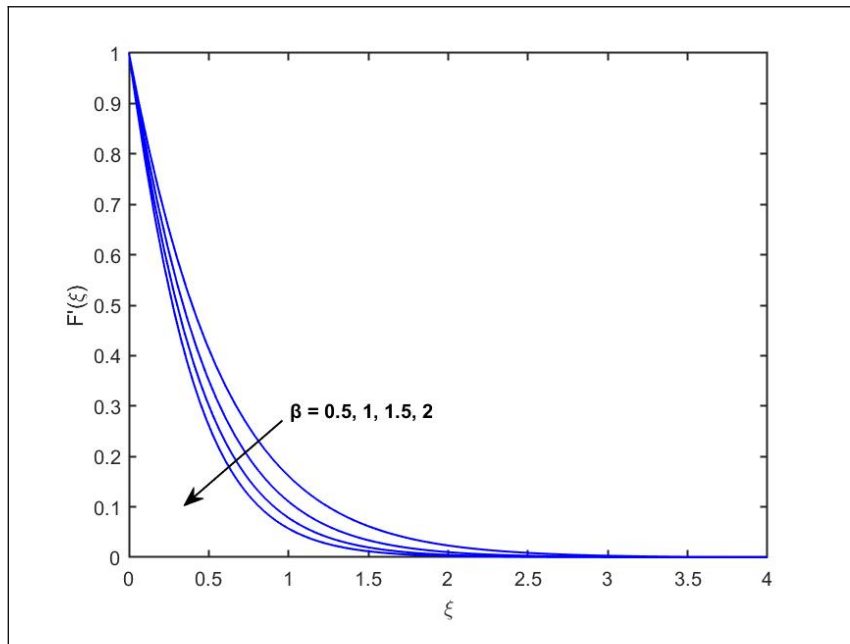


Figure 4.7 (a): Change in $F'(\xi)$ for increasing values of β_1 .

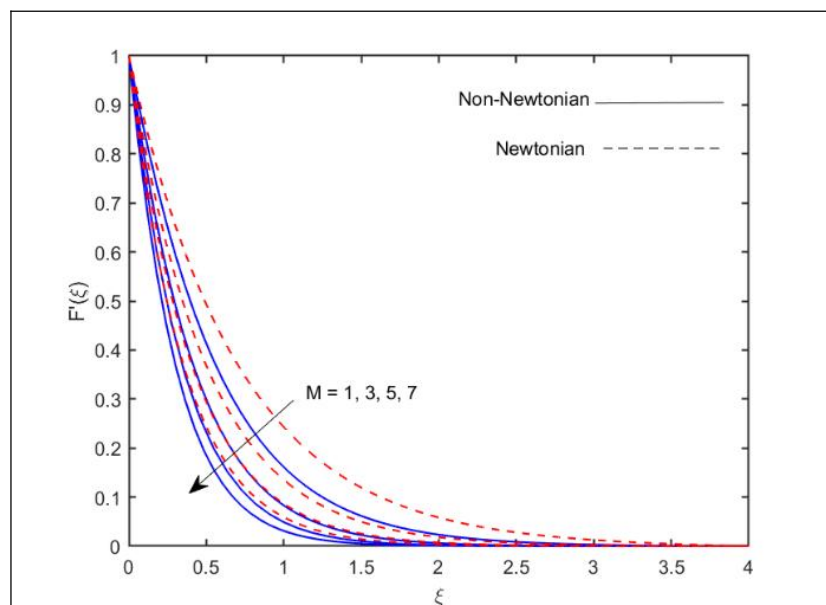


Figure 4.7 (b): Change in $F'(\xi)$ for increasing values of M .

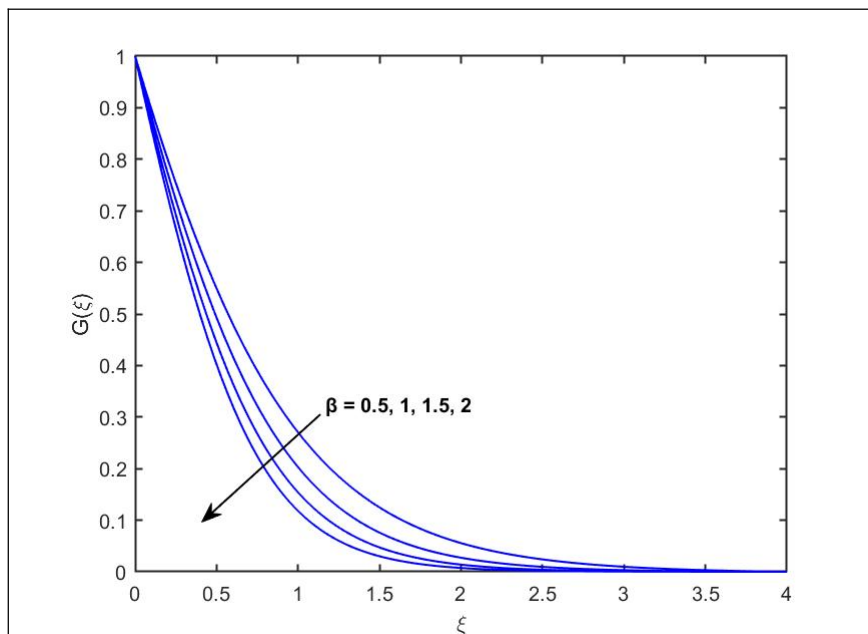


Figure 4.8 (a): Change in $G(\xi)$ for increasing values of β_1 .

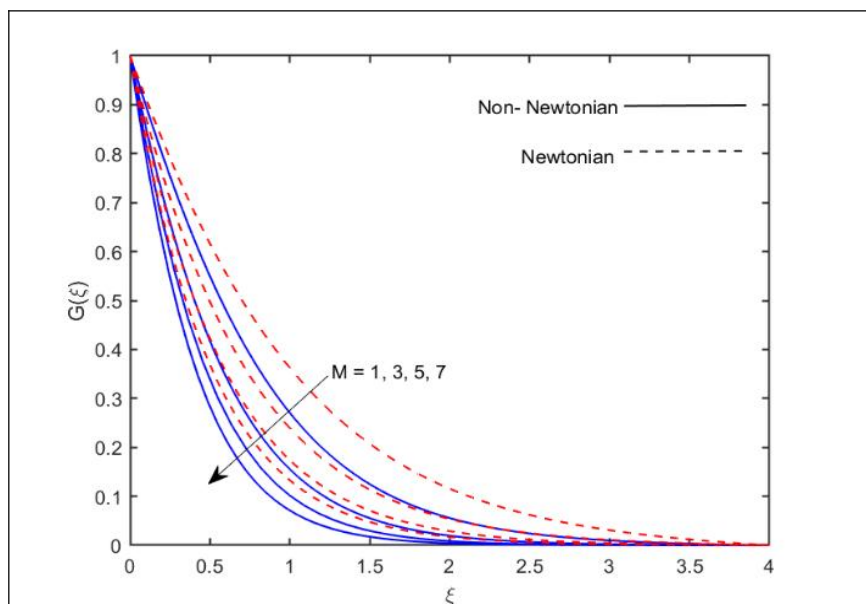


Figure 4.8 (b): Change in $G(\xi)$ for increasing values of M .

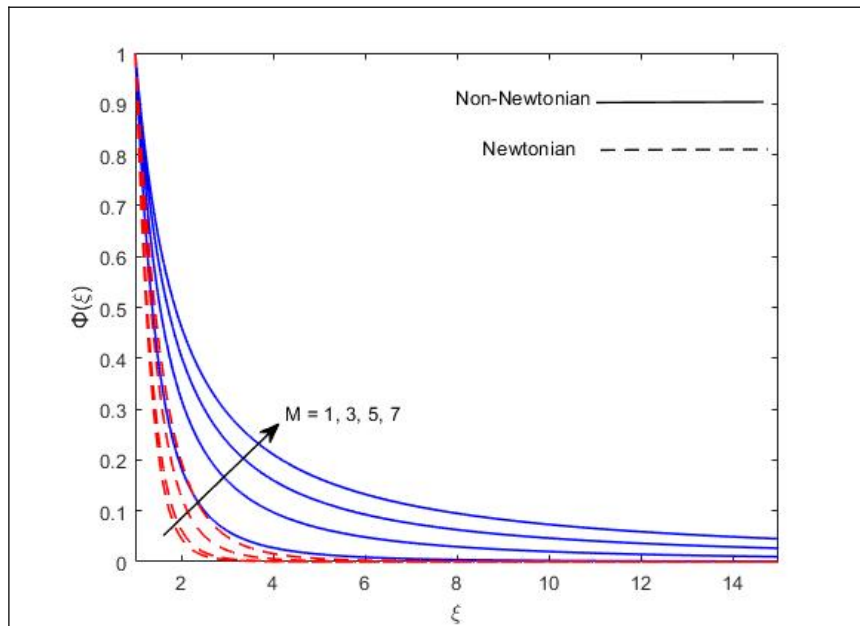


Figure 4.9 (a): Change in $\Phi(\xi)$ for increasing values of M .

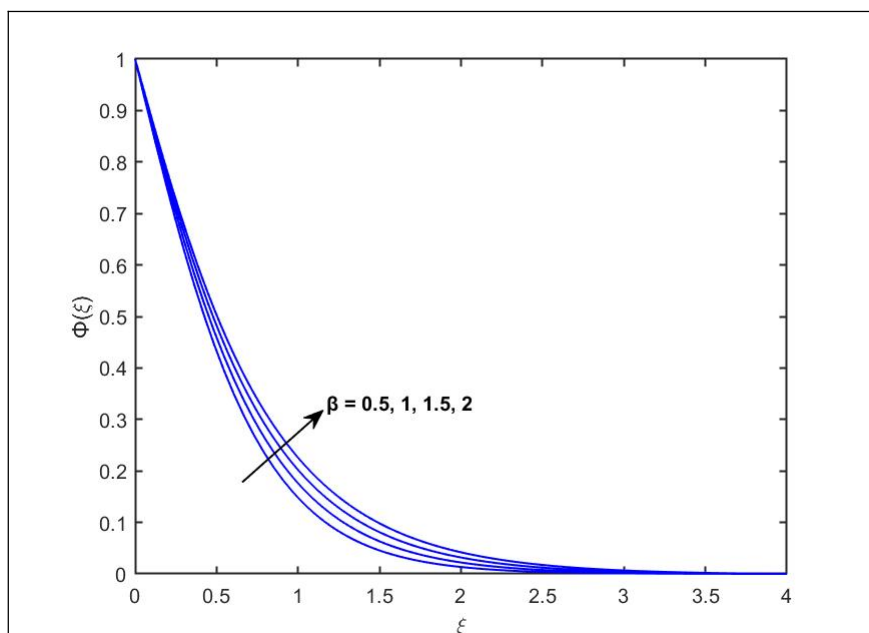


Figure 4.9 (b): Change in $\Phi(\xi)$ for increasing values of β_1 .

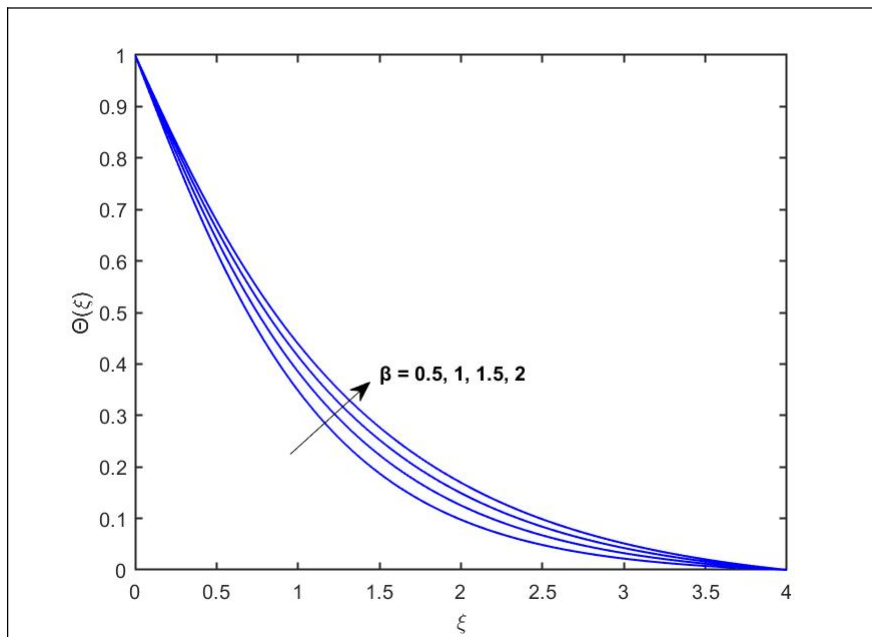


Figure 4.10 (a): Change in $\Theta(\xi)$ for increasing values of β_1 .

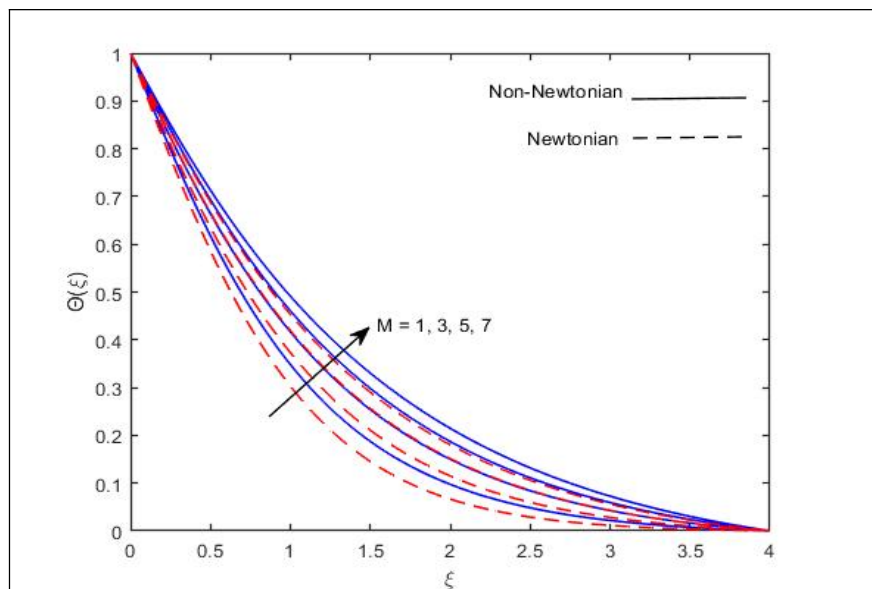


Figure 4.10 (b): Change in $\Theta(\xi)$ for increasing values of M .

Table 1: Numerical data of $-\theta'(0)$ for different values of Re , β_1 , Pr , and $M = 0$.

Re	β_1	Pr	$-\theta'(0)$
01	0.1	4.5	1.122090
02			1.110753
03			1.098944
04			1.087626
01	0.1	4.5	0.474278
	0.2		0.718912
	0.3		0.904159
	0.4		1.059115
01	0.1	01	1.456782
		02	1.417869
		03	1.398765
		04	1.369800

CHAPTER 5

Swirling Flow of Maxwell Fluids with Bioconvection Phenomenon subject to Soret and Dufour Effect

5.1 Introduction

In this chapter, the energy transfer properties in Maxwell fluid flow at stretching and rotating cylinders are examined in detail. The transportation mechanisms are investigated by utilizing the Soret-Dufour theory with axially varying surface temperature of cylinder. The movement of microorganism species is also discussed in this problem. A boundary value problem (BVP) for the flow and transport phenomena utilizes the MATLAB bvp4c package to calculate the mathematical results in graphical form. As opposed to an IVP, a boundary value issue has the possibility of having no solution, a finite number of solutions, or an infinite number of solutions. Therefore, tools for solving BVPs often require users to estimate the intended solution. Flow similarity is also an essential tool for the conversion of the complex physical problem PDEs of mass transport and fluid flow into ordinary differential equations (ODEs). The use of appropriate parameters makes it possible to simulate the complete problem of fluid flow and mass transport, utilizing the partial differential equations. Each result of present study is explained physically in detail. Moreover, the present outcomes are also validated in tabular form with previous published studies.

5.2 Mathematical formulation

Consider the impact of Soret and Dufour effect on the swirling flow of Maxwell fluid along a stretched cylinder of radius R_1 . Suppose that fluid is incompressible and flow is laminar. Moreover, the fluid also contains the microorganism species. Because the cylinder rotates in an axisymmetrically, thus, the equations for the boundary layer in axisymmetric flow

with cylindrical coordinates (r, θ, z) and involve the components of radial, azimuthal and axial velocity (u, v, w) , respectively. The cylinder is considered to rotate around its axis at a constant speed, and the velocity which shows stretching of the cylinder is directly related towards the axial distance. The cylinder's surface temperature and concentration are considered to be T_w and C_w . Also, the concentration of micro-cell species is supposed N_w . Figure 5.1 depicts the flow model's schematic.

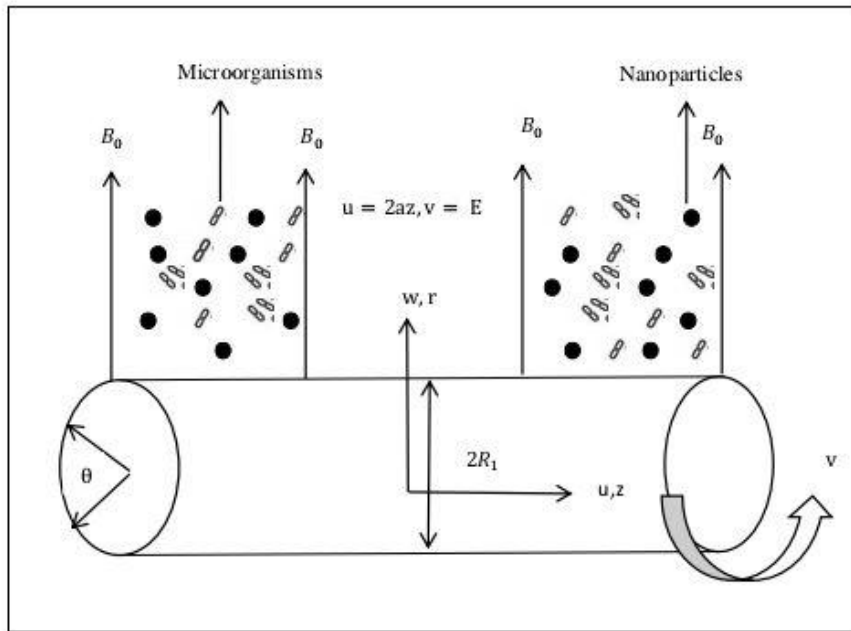


Figure 5.1: Geometry of the problem.

The basic governing equations for the mathematical modeling of present physical problem are:

$$\frac{\partial u}{\partial z} + \frac{w}{r} + \frac{\partial w}{\partial r} = 0, \quad (5.1)$$

$$u \frac{\partial u}{\partial z} + w \frac{\partial u}{\partial r} + \lambda_1 \left[u^2 \frac{\partial^2 u}{\partial z^2} + 2uw \frac{\partial^2 u}{\partial r \partial z} + w^2 \frac{\partial^2 u}{\partial r^2} \right] = -\frac{1}{\rho} \frac{\partial p}{\partial z} + \nu \left[\frac{\partial^2 u}{\partial r^2} + \frac{1}{r} \frac{\partial u}{\partial r} \right] - \frac{\sigma B_0^2}{\rho} \left(u + \lambda_1 w \frac{\partial u}{\partial r} \right), \quad (5.2)$$

$$u \frac{\partial u}{\partial z} + w \frac{\partial u}{\partial r} + \frac{wv}{r} + \lambda_1 \left(u^2 \frac{\partial^2 u}{\partial z^2} + 2uw \frac{\partial^2 u}{\partial r \partial z} + w^2 \frac{\partial^2 u}{\partial r^2} + \frac{2wv}{r} \frac{\partial w}{\partial r} + \frac{2uv}{r} \frac{\partial w}{\partial z} - \frac{2w^2 v}{r^2} \right) = v \left(\frac{\partial^2 v}{\partial r^2} - \frac{v}{r^2} + \frac{1}{r} \frac{\partial u}{\partial r} \right) - \frac{\sigma B_0^2}{\rho} \left(v + \lambda_1 w \frac{\partial v}{\partial r} - \lambda_1 \frac{wv}{r} \right), \quad (5.3)$$

$$u \frac{\partial T}{\partial z} + w \frac{\partial T}{\partial r} = \alpha_1 \frac{1}{r} \frac{\partial}{\partial r} \left(r \frac{\partial T}{\partial r} \right) + \frac{D_T k_T}{C_p C_s} \frac{1}{r} \frac{\partial}{\partial r} \left(r \frac{\partial C}{\partial r} \right), \quad (5.4)$$

$$u \frac{\partial C}{\partial z} + w \frac{\partial C}{\partial r} = D_B \frac{1}{r} \frac{\partial}{\partial r} \left(r \frac{\partial C}{\partial r} \right) + \frac{D_T k_T}{T_\infty} \frac{1}{r} \frac{\partial}{\partial r} \left(r \frac{\partial T}{\partial r} \right), \quad (5.5)$$

$$u \frac{\partial N}{\partial z} + w \frac{\partial N}{\partial r} + \frac{bW_c}{C_w - C_\infty} \left[\frac{\partial N}{\partial r} \frac{\partial C}{\partial r} + N \frac{\partial^2 C}{\partial r^2} \right] = D_m \left[\frac{\partial^2 N}{\partial r^2} + \frac{1}{r} \frac{\partial N}{\partial r} \right], \quad (5.6)$$

For the specified flow problem, the boundary conditions are

$$\left. \begin{aligned} u(z, r) = 2az, v(z, r) = E, w(z, r) = 0, T = T_w, C = C_w, N = N_w \text{ at } r = R_1 \\ u = 0, v = 0, T = T_\infty, C = C_\infty, N = N_\infty \text{ as } r \rightarrow \infty. \end{aligned} \right\} \quad (5.7)$$

The kinematic viscosity represents by ν , thermal diffusivity denoted by α_1 , $a > 0$ specify the strength of the cylinder's stretching, while E denotes the cylinder's constant torsion and has the same dimensions as velocity. Fluid stress relaxation time, defines by λ_1 , diffusion coefficients for thermal and solutal energy transport express as D_T and D_B , respectively.

In Eq. (5.6) W_c is the highest swimming velocity of microorganism, b the chemotaxis parameter and D_m the diffusion coefficient of microorganism species.

The governing equations can be simplified into ordinary differential equations with following variables.

$$u = 2azf'(\eta), v = Eg(\eta), w = -aR_1 \frac{f(\eta)}{\eta^2}, \quad (5.8)$$

$$\theta(\eta) = \frac{T - T_\infty}{T_w - T_\infty}, \quad \theta(\eta) = \frac{T - T_\infty}{bz}, \quad \phi(\eta) = \frac{C - C_\infty}{C_w - C_\infty}, \quad h(\eta) = \frac{N - N_\infty}{N_w - N_\infty} \quad \text{and} \quad \eta = \frac{r^2}{R_1^2}$$

When the above substitution are used

$$\eta f'''' + f'' + Re f f'' - Re f'^2 - \beta_1 Re \left(\frac{f^2 f''}{\eta} + 2f^2 f''' + 4ff'f'' \right) - MRe \left(\frac{f'}{2} - \beta_1 f f'' \right) = 0, \quad (5.9)$$

$$2\eta^2 g'' + 2\eta g' - \frac{g}{2} + 2Re\eta f g' + Refg - \beta_1 Re \left(2f^2 g' + 4\eta f^2 g'' - 4ff'g - \frac{4f^2 g}{\eta} \right) - MRe \left(g - 2\beta_1 f g' - \beta_1 \frac{fg}{\eta} \right) = 0, \quad (5.10)$$

$$\frac{1}{RePr} [2\theta' + 2\eta\theta''] + \frac{Du}{Re} [2\phi' + 2\eta\phi''] + f\theta' = 0, \quad (CWT) \quad (5.11)$$

$$\frac{1}{RePr} [2\theta' + 2\eta\theta''] + \frac{Du}{Re} [2\phi' + 2\eta\phi''] - f'\theta + f\theta' = 0, \quad (PST) \quad (5.12)$$

$$\frac{1}{LeRe} [2\eta\phi'' + 2\phi'] + \frac{Sr}{Re} [2\eta\theta'' + 2\theta'] + f\theta' = 0, \quad (5.13)$$

$$\frac{1}{LbRe} [2h' + 2\eta h''] + \frac{Pe}{LbRe} [2\phi' h' + 2\phi'' h + 2N_g \phi''] + fh' = 0 \quad (5.14)$$

With boundary conditions

$$\left. \begin{aligned} f(0) = 0, \quad f'(0) = 1, \quad g(0) = 1, \quad \theta(0) = 1, \quad \phi(0) = 1, \quad h(0) = 1 \\ \lim_{x \rightarrow \infty} e^{-x} f(\infty) = 0, \quad g(\infty) = 0, \quad \theta(\infty) = 0, \quad \phi(\infty) = 0, \quad h(\infty) = 0. \end{aligned} \right\} \quad (5.15)$$

Thus, following the Fang [4] to make convergence fast the variable η transformed as e^x .

$$f_{xxx} - 2f_{xx} + f_x - Re(f_x^2 - ff_{xx} + ff_x) - \beta_1 Re e^{-x} (2f^2 f_{xxx} - 5f^2 f_{xx} + 3f^2 f_x - 4ff_x^2) - MRe \left(e^x \frac{f_x}{2} - \beta_1 ff_{xx} + \beta_1 ff_x \right) = 0, \quad (5.16)$$

$$2g_{xx} - \frac{g}{2} + Re(2fg_x + fg) - \beta_1 Re e^{-x} (6f^2 g_x + 4f^2 g_{xx} + 4ff_x g - 4f^2 g) - MRe (g - 2\beta_1 e^{-x} f g_x - \beta_1 e^{-x} f g) = 0, \quad (5.17)$$

$$\frac{1}{RePr} \theta_{xx} + \frac{Du}{Re} \phi_{xx} + \frac{f}{2} \theta_x = 0, \quad (5.18)$$

$$\frac{1}{RePr} \theta_{xx} + \frac{Du}{Re} \phi_{xx} - \frac{f_x \theta}{2} + \frac{f \theta_x}{2} = 0, \quad (5.19)$$

$$\frac{1}{LeRe} \phi_{xx} + \frac{Sr}{Re} \theta_{xx} + \frac{f}{2} \phi_x = 0, \quad (5.20)$$

$$\frac{1}{LbRe} h_{xx} + \frac{Pe}{LbRe} e^{-x} [2h_x \phi_x + \phi_{xx} (h + N_g)] + \frac{f}{2} h_x = 0, \quad (5.21)$$

With boundary conditions

$$\left. \begin{aligned} f(0) = 0, \quad f_x(0) = 1, \quad g(0) = 1, \quad \theta(0) = 1, \quad \phi(0) = 1, \quad h(0) = 1 \\ \lim_{x \rightarrow \infty} e^{-x} f(\infty) = 0, \quad g(\infty) = 0, \quad \theta(\infty) = 0, \quad \phi(\infty) = 0, \quad h(\infty) = 0. \end{aligned} \right\} \quad (5.22)$$

Dimensionless parameters are expressed as:

$$\begin{aligned} Re &= \left(\frac{aR_1^2}{2v} \right), \quad Sc = \left(\frac{v}{D_m} \right), \quad Pr = \left(\frac{v}{\alpha_1} \right), \quad Le = \left(\frac{\alpha_1}{D_B} \right), \quad Du = \frac{D_T K_T}{V C_p C_S} \left(\frac{C_W - C_\infty}{T_W - T_\infty} \right) \\ \beta &= (\lambda_1 a), \quad M = \left(\frac{\sigma B_0^2}{\rho a} \right), \quad Pe = RePr, \quad Sr = \frac{D_T K_T}{T_\infty} \left(\frac{T_W - T_\infty}{C_W - C_\infty} \right) \end{aligned} \quad (5.23)$$

The Reynolds number is denoted by Re , while the Schmidt number is represented by Sc . In addition, the Deborah number is represented by β , Du stands for the Dufour number, M represents the magnetic field parameter, Pe is the Peclet number, the Soret number is denoted by Sr , the Prandtl number is represented by Pr , and finally, the Lewis number is represented by Le .

5.3 Method of Solution

This part is recommended for the solution of well-known ODEs for flow, temperature, concentration, and concentration of Microorganisms equations numerical scheme. The first order ODEs can be computed by using bvp4c method. Thus, the variables are assumed as:

$$f = y_1, \quad f_x = y_2, \quad f_{xx} = y_3, \quad f_{xxx} = yy_1, \quad (5.24)$$

$$g = y_4, \quad g_x = y_5, \quad g_{xx} = yy_2, \quad (5.25)$$

$$\theta = y_6, \quad \theta_x = y_7, \quad \theta_{xx} = yy_3, \quad (5.26)$$

$$\phi = y_8, \quad \phi_x = y_9, \quad \phi_{xx} = yy_4, \quad (5.27)$$

$$h = y_{10}, \quad h_x = y_{11}, \quad h_{xx} = yy_5, \quad (5.28)$$

$$yy_1 = \frac{(2y_3 - y_2 + Rey_3y_3 - y_2y_3y_1y_2) + BRe \times e^{-x}[3y_1y_1y_2 - 5y_1y_1y_3 - 4y_1y_2y_3 + 4y_1y_2y_2 + MRe(e^{-x}y_2 - By_1y_3)]}{a_1}, \quad (5.29)$$

$$yy_2 = \frac{\left[\left(\frac{y_4}{2} \right) - 2Rey_1y_5 - Rey_1y_4 + BRee^{-x}(2y_1y_1y_5 - 4y_1y_1y_5 + 4y_1y_2y_4 - 4y_1y_1y_4) + MRe(y_4 - 2Be^{-x}y_1y_5 - Be^{-x}y_1y_4) \right]}{b_1} \quad (5.30)$$

$$yy_3 = \frac{\left(-Pr \times De^{\frac{-Re \times Pr \times Le \times y_1 y_9}{2}} \right) \frac{Re \times Pr \times y_1 y_7}{2}}{c_1}, \quad (5.31)$$

$$yy_3 = \frac{\left(-Pr \times De^{\frac{-Re \times Pr \times Le \times y_1 y_9}{2}} \right) \frac{Re \times Pr \times y_1 y_7}{2} + \frac{Re \times Pr \times y_2 y_6}{2}}{c_1}, \quad (5.32)$$

$$yy_4 = \frac{-Ds \times Pr \times Le \times y_3 - Re \times Pr \times Le \times y_1 \times y_9}{2}, \quad (5.33)$$

$$yy_5 = \frac{-Pe \times e^{-x}(y_{11}y_9 + (yy_4 - y_9)(y_{10} + N_g) - Re Sby_1y_{11})}{2}, \quad (5.34)$$

where

$$a_1 = (1 - 2 \times B \times Re \times e^{-x} \times y_1 \times y_1), \quad b_1 = (2 - 4 \times B \times e^{-x} \times Re \times y_1 \times y_1) \quad \text{and}$$

$$c_1 = 1 + Ds \times Pr \times Le,$$

$$\begin{aligned} y_1(0) &= 0, & y_2(0) &= 1, & y_4(0) &= 1, & y_6(0) &= 1, & y_8(0) &= 1, & y_{10}(0) &= 1 \\ y_1(\infty) &= 0, & y_4(\infty) &= 0, & y_6(\infty) &= 0, & y_8(\infty) &= 0, & y_{10}(\infty) &= 0. \end{aligned} \quad (5.35)$$

5.4 Results and Discussion

The numerical conclusions for temperature, concentration and microbial concentration profiles with velocity are explored using graphs. The effect of Reynolds number Re , magnetic parameter M , Maxwell parameter β_1 on the velocity and Soret number Sr , Lewis number Le , Dufour number Du on temperature, and concentration fields is provided visually by

comparing (PST) prescribed surface temperature and (CWT) constant wall temperature. Figs. 5.2 (a – c) represent the velocity components for greater values of Reynolds numbers Re , Maxwell Parameter β_1 and magnetic parameter M . The results show that the fluid velocity decreases exponentially for the Reynolds number, Maxwell parameter, and magnetic parameter. Figs. 5.3 represent the velocity components for greater values of Reynolds number Re and magnetic number M . Greater values of Re and M reduce velocity. Figs. 5.2 (a) and 5.3 (a) show a decrease in Reynolds number with an increase in the velocity profile. As the Reynolds number increases, viscous forces become less prominent, and consequently, velocity defects in the flow field propagate less. Fig. 5.2 (b) shows an increase in Maxwell number and a decrease in the velocity profile. When the Maxwell parameter β_1 reaches higher values, there is an increase in stress relaxation in viscoelastic fluids. This causes the liquid to take on a more solid-like quality, decreasing fluid motion. The influence of the magnetic parameter (M) on the velocity profiles is seen in Figs. 5.2 (c) and 5.3 (b). With the increase in magnetic parameter, the velocity profiles decrease. The induced Lorentz force in the boundary layer increases with an increase in the magnetic parameter, and as a result, the velocity profiles also increase. This demonstrates that increasing the magnetic parameter increases the Lorentz force, and hence this force reduces fluid velocity within the boundary layer. Variation in the temperature profile, which is essentially the heat transfer distribution. Figures 5.4 (a – f) show the impact of several factors, including the Maxwell parameter, Soret number Sr , Dufour parameter Du , Lewis number Le , Magnetic number M , Prandtl number Pr and Reynolds number Re on the temperature field in the presence of motile microorganisms. Fig. 5.4 (a) shows boost-up in thermal field with higher values of the Maxwell parameter. Because of the stress relaxation phenomenon, elastic strain gradually converts to plastic strain, and the liquid becomes more solid-like, resulting in an increase in thermal energy. Figs. 5.4 (b) and (c) show the impact of Soret and Dufour numbers on temperature. With the increasing values of the Soret number, the temperature also increases. The Soret number is the variation in temperature divided by the concentration. Dufour number also increases with an increase in temperature. Fig. 5.4 (d) shows that higher values of the Lewis number result in an increase in temperature. As the Lewis number is the ratio between thermal and mass diffusion rates, with an increase in the Lewis number, the temperature also increases. As it represents the proportional relationship between heat and mass diffusion rates. Fig. 5.4 (e) shows an increase in temperature profile with increasing values of the magnetic parameter. Fig. 5.4 (f) shows a decrease in temperature profile with increasing values of the Prandtl number. With increasing values of the Prandtl number, the temperature decreases. As Prandtl number is obtained by dividing momentum

diffusivity by thermal diffusivity. Increasing values of Prandtl number Pr reduce the temperature field due to the fluid's reduced thermal diffusivity. Fig. 5.4 (g) shows that for increasing values of the Reynolds number, the temperature decreases. Figs. 5.5 (a, b) show the impact of magnetic number and Reynolds number on concentration. The Reynolds number decreases with an increase in concentration, which increases as a result of an increase in viscosity. As viscous force increases, with a decrease in Reynolds number. The concentration profile of the fluid, on the other hand, increases significantly with an increasing value of a magnetic parameter. Concentration plays a significant role in altering the Soret number and Dufour number, as demonstrated in Figs. 5.5 (c, d). A higher concentration corresponds to a higher Soret number, while the Dufour number decreases as concentration increases.

Figure 5.6 shows the impact of different parameters on the concentration of microorganisms. Fig. 5.6 (a) shows an increase in the concentration of microorganisms with increasing values of a magnetic parameter. Fig. 5.6 (b) shows a decrease in the concentration of microorganisms with increasing values of the Reynolds number. Fig. 5.6 (c) shows a decrease in microorganism concentration with the increase in bioconvection Schmidt number. The Schmidt number of bioconvection Sb , is the ratio of momentum diffusivity to microorganism diffusivity. As this parameter grows, the difference in diffusivity increases, and the momentum diffusion rate gradually replaces the microorganism diffusion rate, resulting in a decrease in microorganism concentration. Figs. 5.6 (d, e) show the concentration of microorganisms with Peclet number Pe and bioconvection Lewis number Lb . The microbe concentration curves show that the microorganism concentration increases with the increase in Peclet number and bioconvection Lewis number. Due to the ratio of gyrotactic microorganisms' momentum to mass diffusivities, the bioconvection Lewis number is produced. Diffusivities like these lead to an increase in the concentration of gyrotactic bacteria. The increasing value of the Peclet number decreases the molecular diffusion rate, causing an increase in the concentration profile of motile microorganisms. Fig. 5.6 f shows the effect of microorganism parameter on concentration of microorganisms. Microorganism parameter decreases with an increase in concentration of microorganisms. The tabular data in table 2 is provided in order to validate the outcomes of this investigation. This data shows the numeric values of velocity gradient at the surface of cylinder.

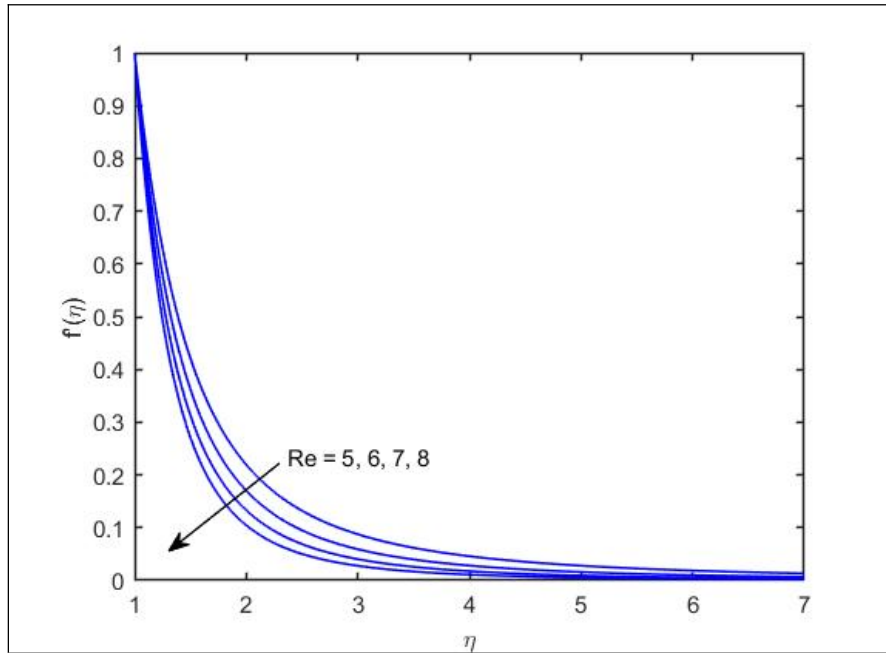


Figure 5.2 (a): Variation in $f'(\eta)$ for increasing values Re .

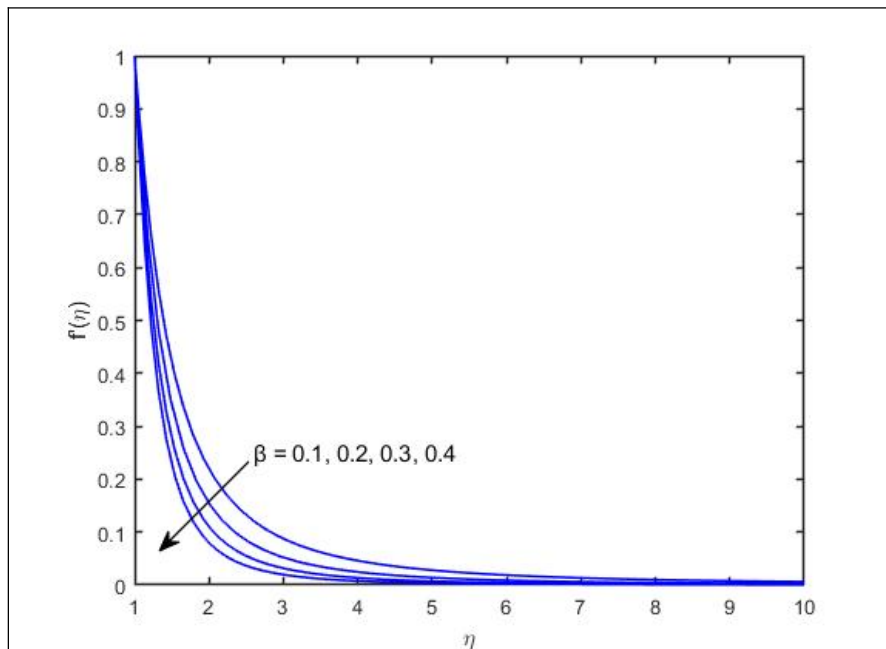


Figure 5.2 (b): Variation in $f'(\eta)$ for increasing values β_1 .

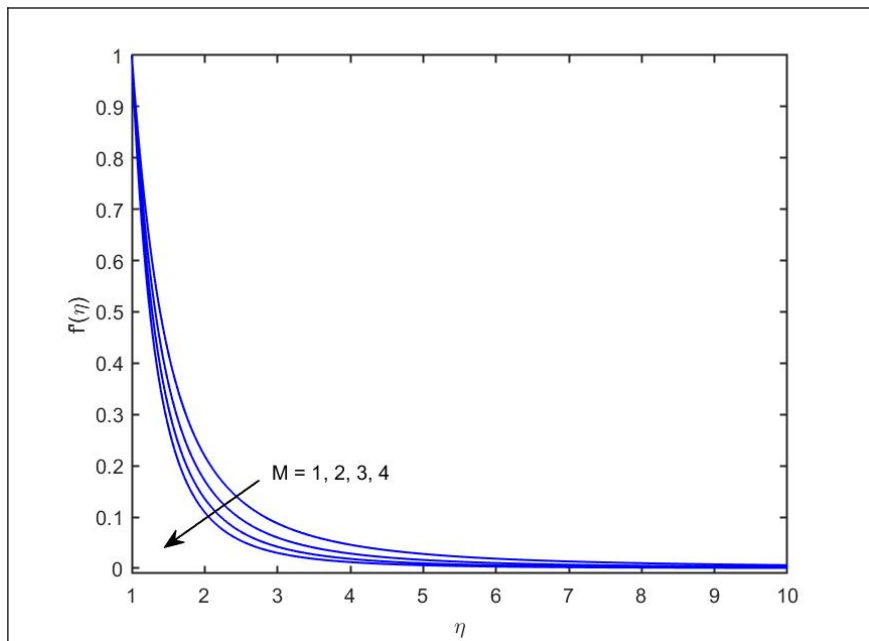


Figure 5.2 (c): Variation in $f'(\eta)$ for increasing values M .

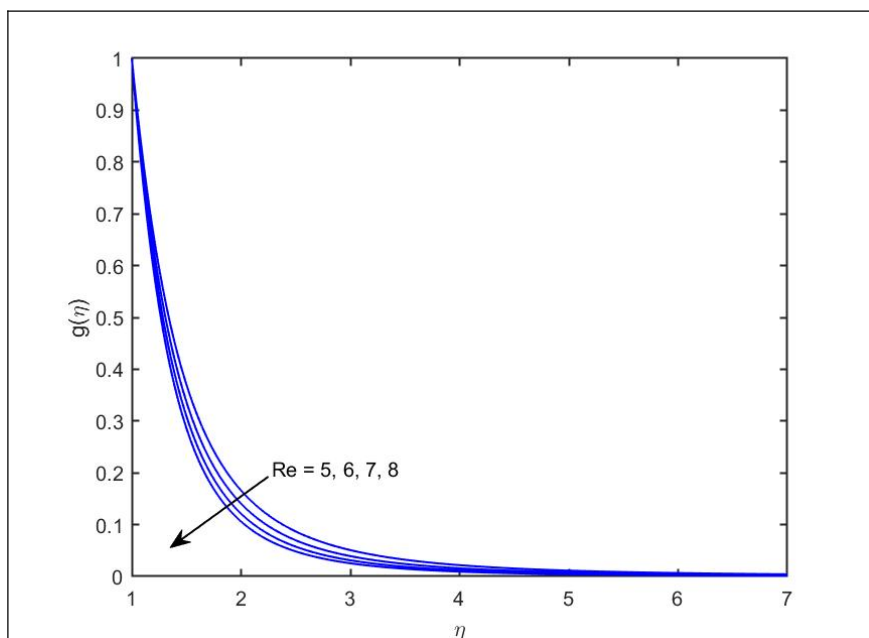


Figure 5.3 (a): Variation in $g(\eta)$ for increasing values of Re .

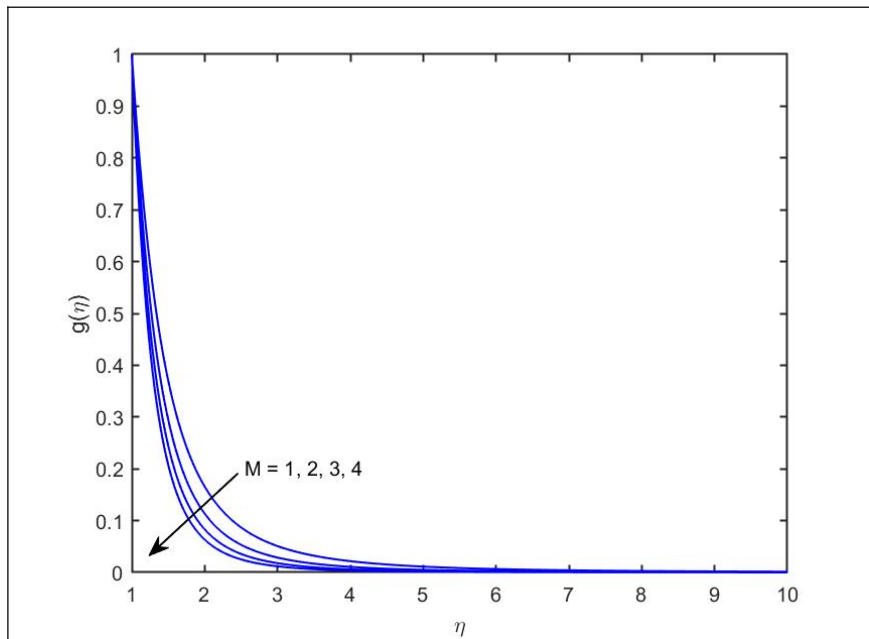


Figure 5.3 (b): Velocity component $g(\eta)$ for increasing values of M .

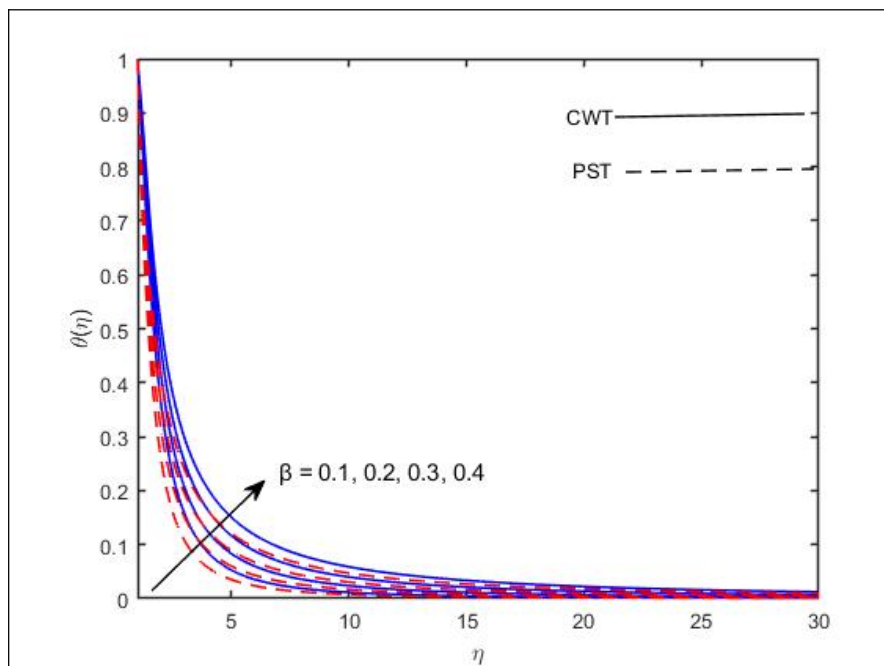


Figure 5.4 (a): Change in $\theta(\eta)$ for increasing values of β_1 .

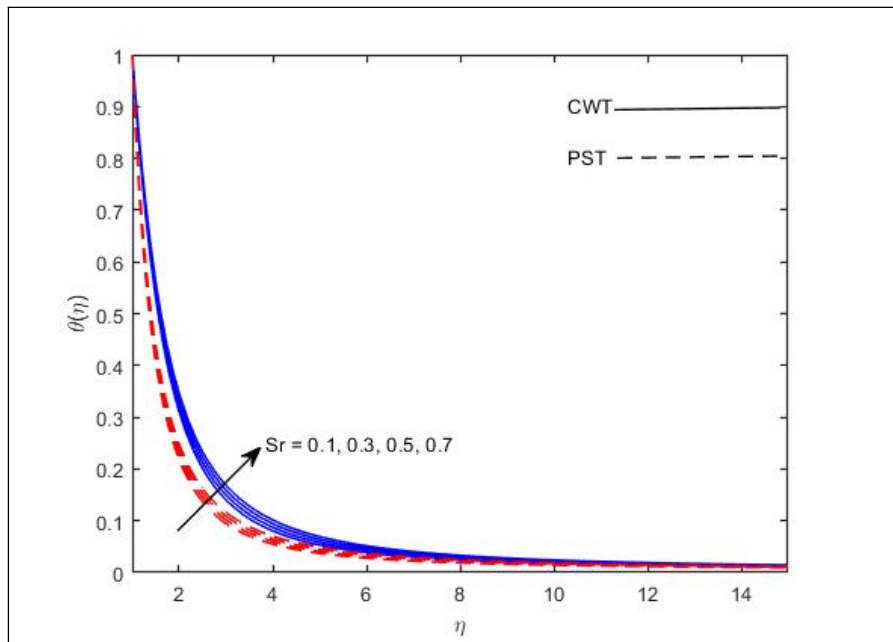


Figure 5.4 (b): Temperature profile $\theta(\eta)$ for increasing values of Sr .

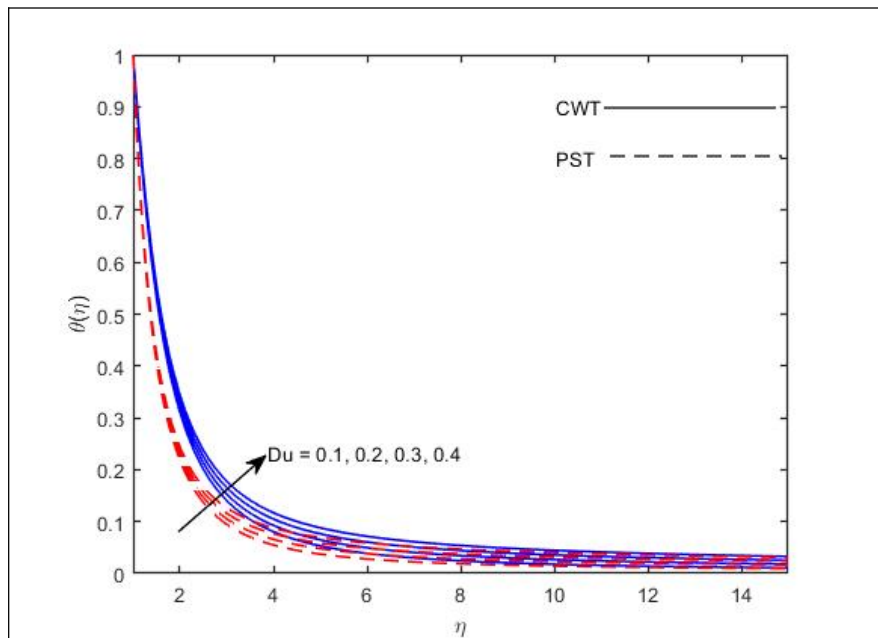


Figure 5.4 (c): Change in $\theta(\eta)$ for higher values of Du .

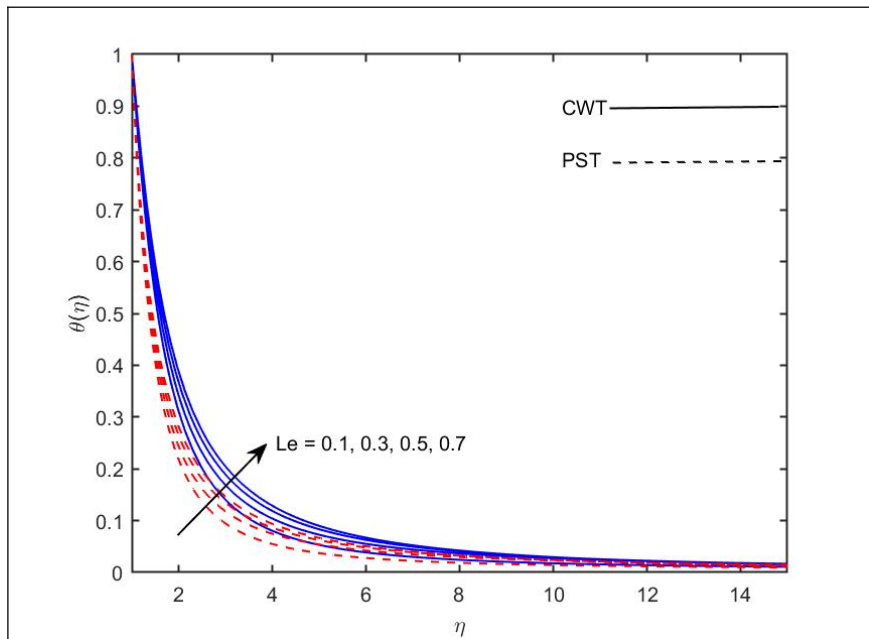


Figure 5.4 (d): Change in $\theta(\eta)$ for increasing values of Le

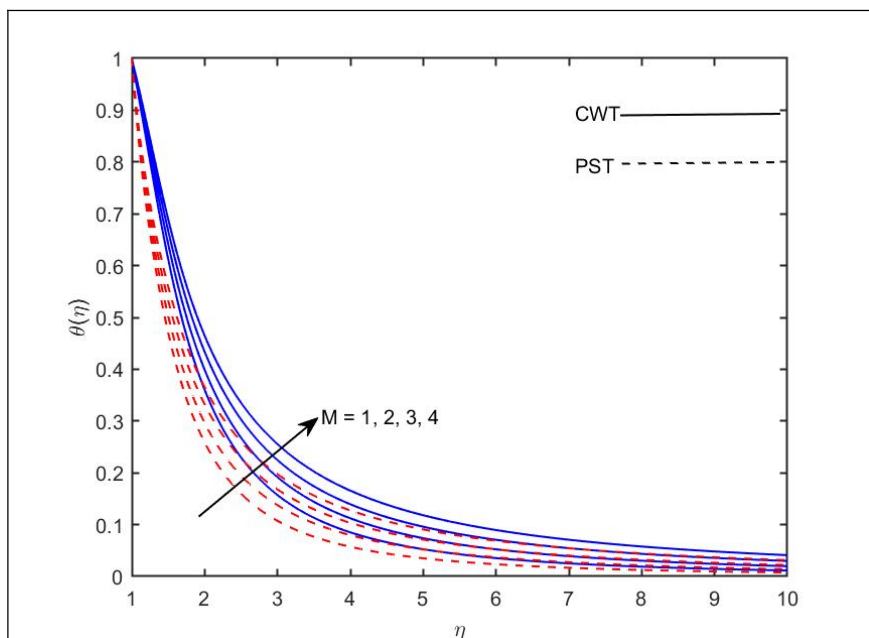


Figure 5.4 (e): Variation in $\theta(\eta)$ for more values of M

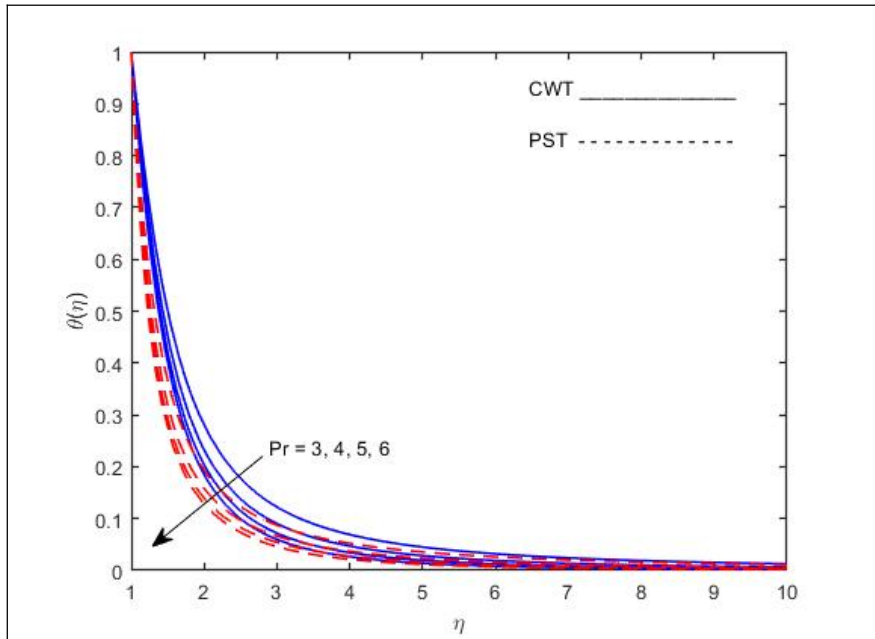


Figure 5.4 (f): Variation in $\theta(\eta)$ for large values of Pr .

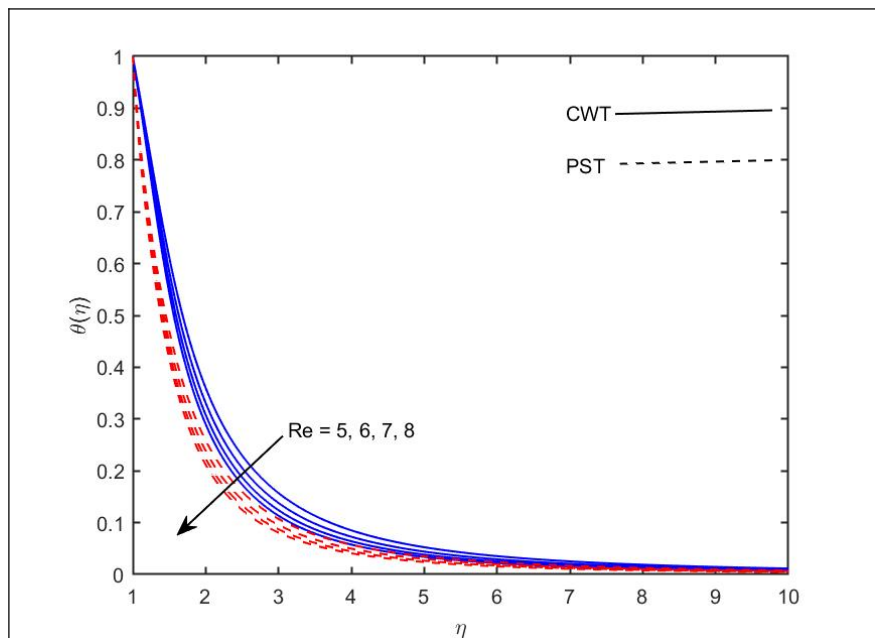


Figure 5.4 (g): Trend of $\theta(\eta)$ for increasing values of Re .

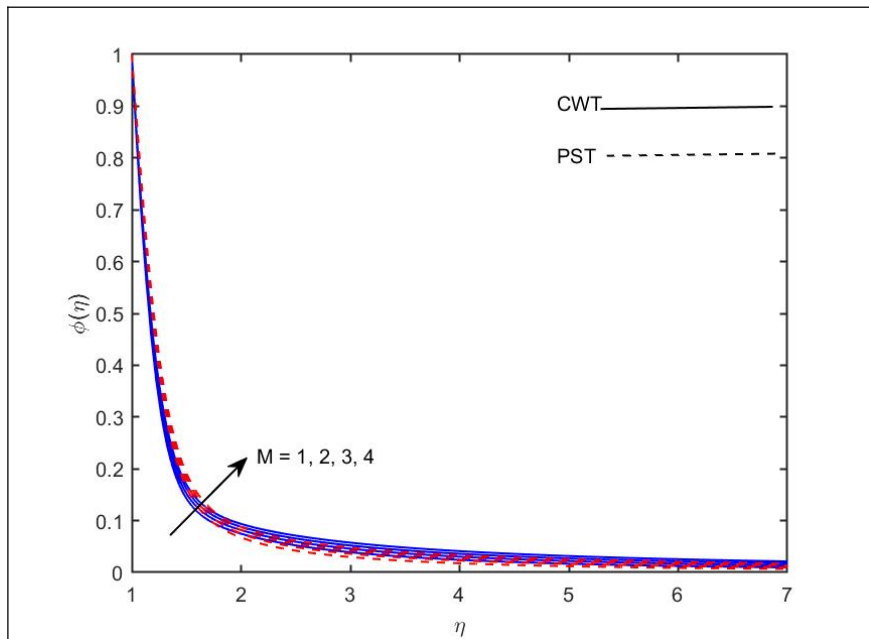


Figure 5.5 (a): Magnetic field impact on in $\phi(\eta)$.

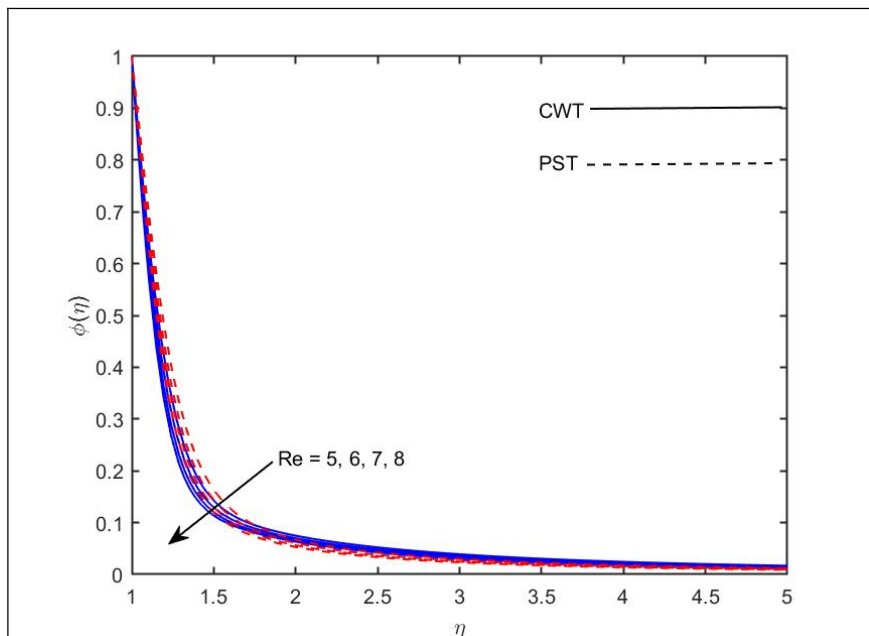


Figure 5.5 (b): Behaviour of $\phi(\eta)$ for increasing values of Re .

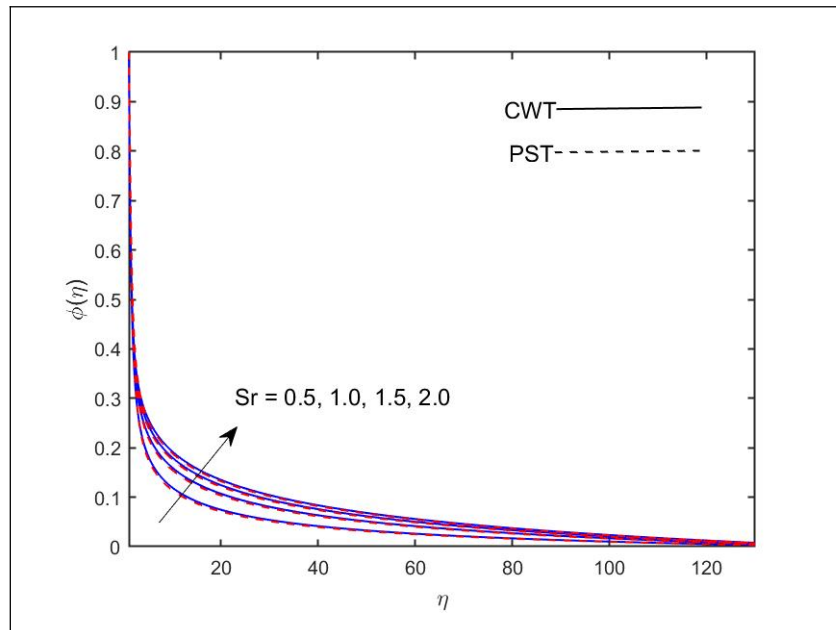


Figure 5.5 (c): Behaviour of $\phi(\eta)$ for more values of Sr .

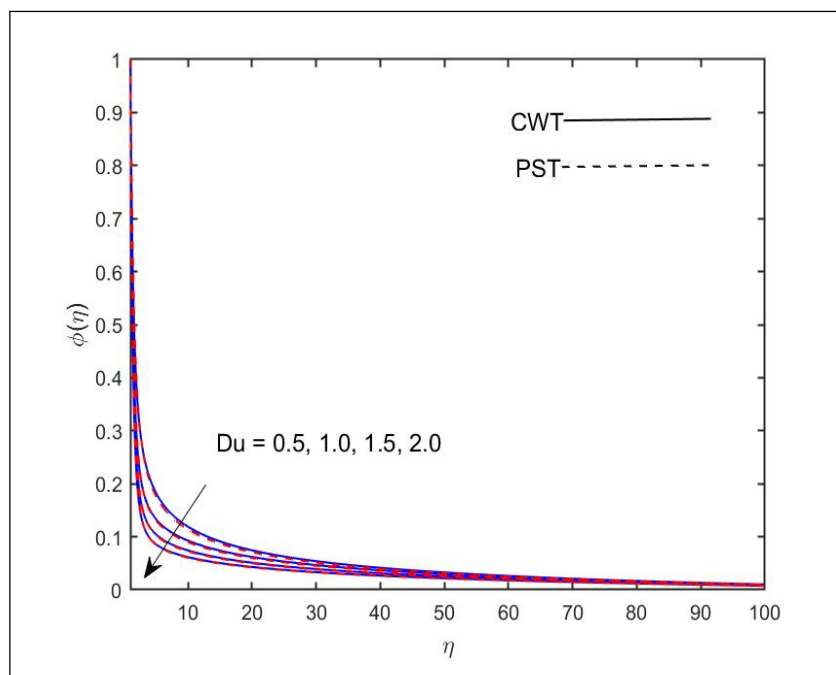


Figure 5.5 (d): Behaviour of $\phi(\eta)$ for the values of Du .

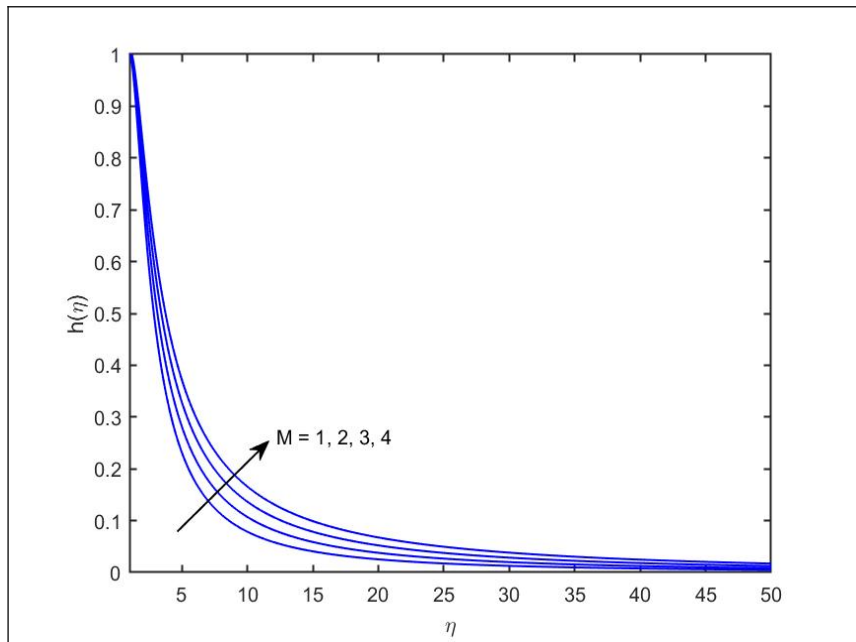


Figure 5.6 (a): Trend of $h(\eta)$ for more values of M .

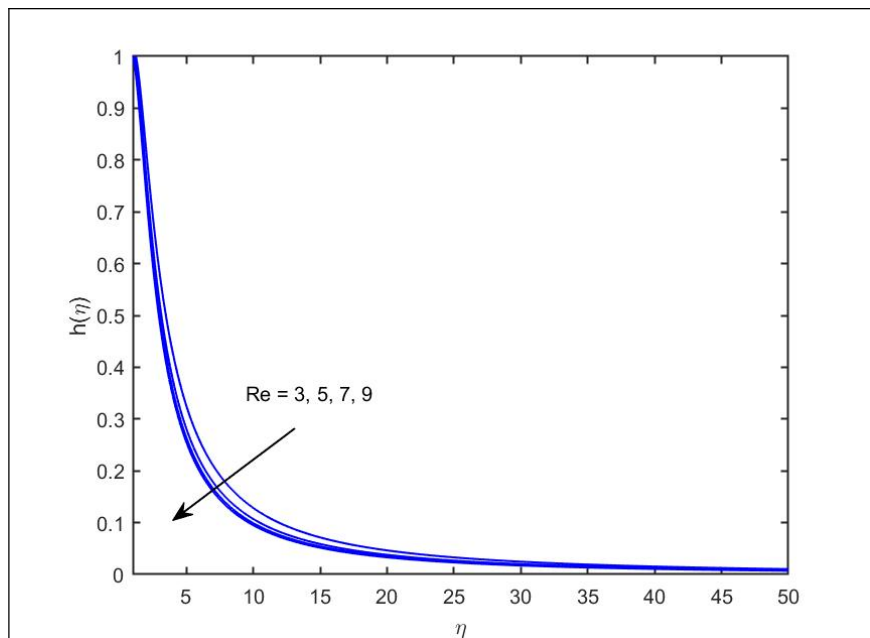


Figure 5.6 (b): Trend of $h(\eta)$ for increasing values of Re .

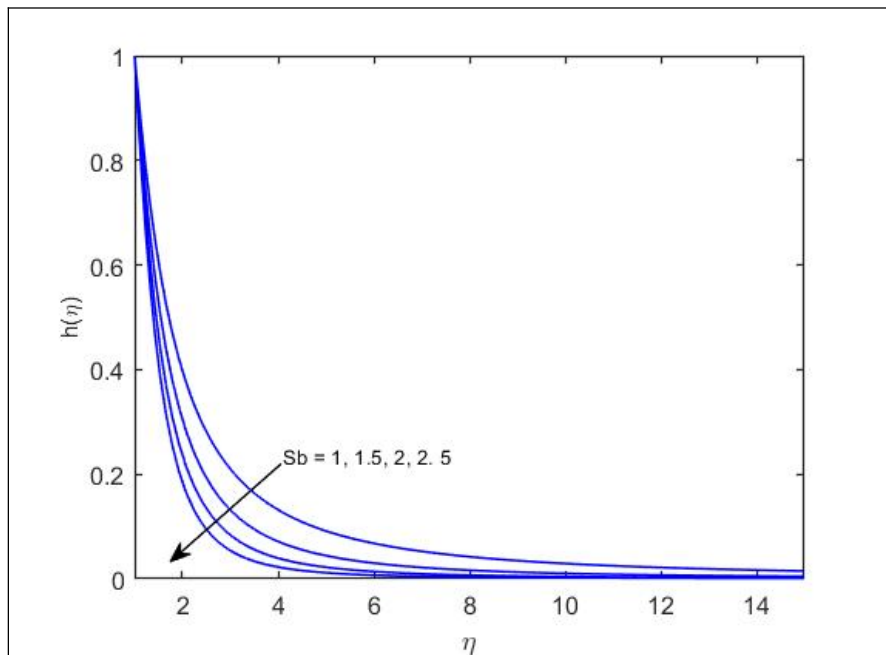


Figure 5.6 (c): Trend of $h(\eta)$ for higher values of S_b .

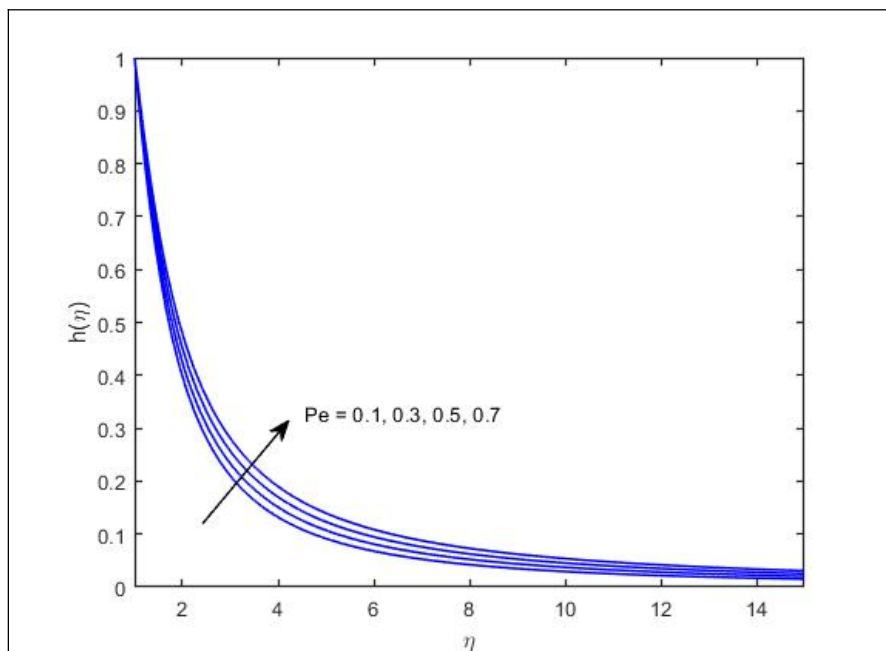


Figure 5.6 (d): Variation in $h(\eta)$ for higher values of Pe .

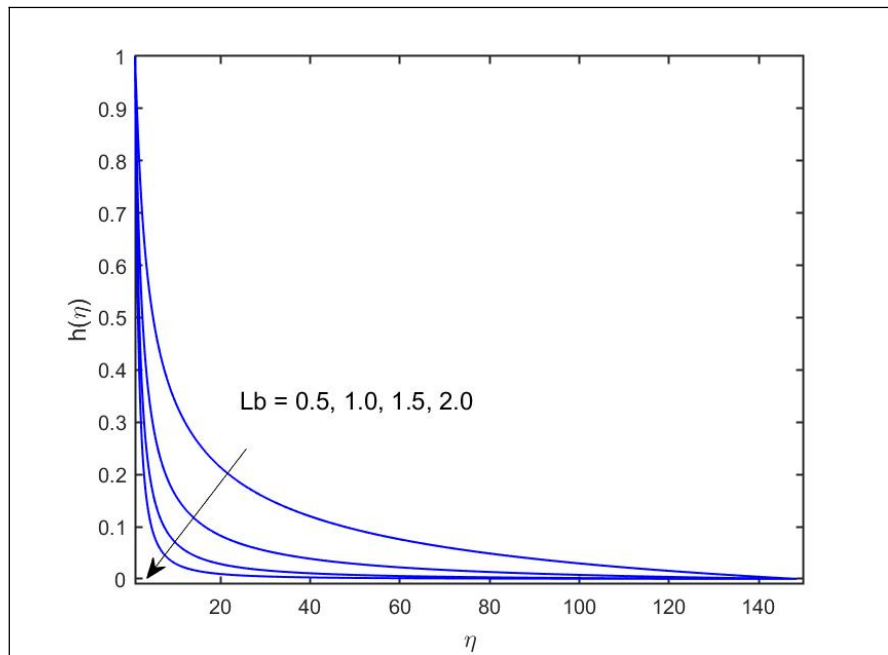


Figure 5.6 (e): Variation in $h(\eta)$ for various values of Lb .

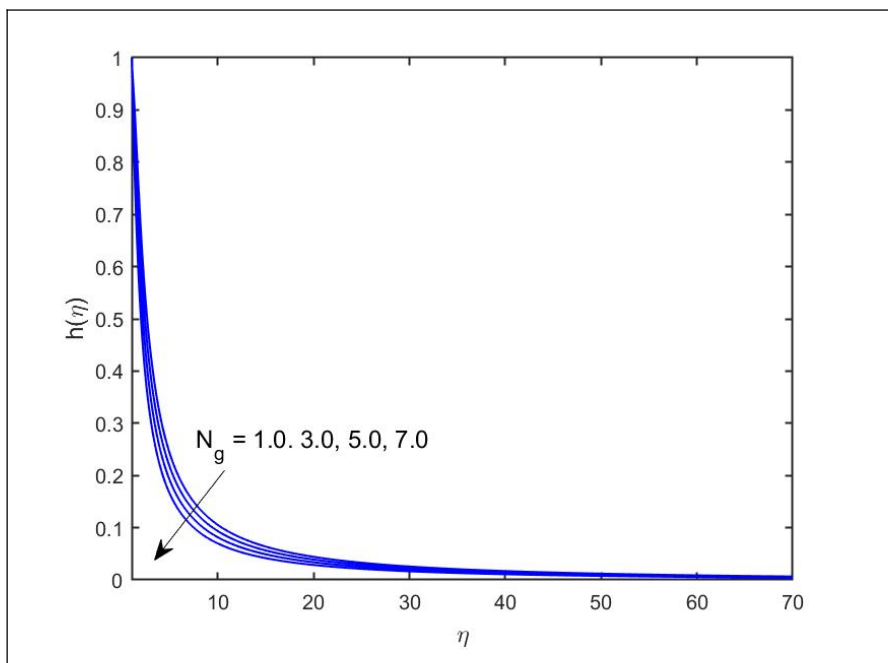


Figure 5.6 (f): Variation in $h(\eta)$ for higher values of N_g .

Table 2 : Numerical values of $f'(1)$ and $g'(1)$ for various of Re in case when $\beta_1 = M = 0$.

Re	$f''(1)$	$g'(1)$	$f''(1)$	$g'(1)$
	Ref.[63]	Ref.[63]	Present numerics	Present numerics
0.1	- 0.48180	- 0.51019	-0.488807	-0.501242
0.2	- 0.61748	- 0.52605	-0.610123	-0.528009
0.3			-0.711362	-0.563163
0.4			-0.797318	-0.585519
0.5	- 0.88220	- 0.58488	-0.809641	-0.608361
01	- 1.17775	- 0.68772	-1.177369	-0.697271
02	- 1.59389	- 0.87263	-1.596940	-0.869005
03			-1.911386	-1.038014

CHAPTER 6

CONCLUSIONS AND FUTURE WORK

This research work was established to investigate the rheological features of the swirling flow of Maxwell fluid around a stretchable cylinder. The bioconvection phenomenon, under the influence of the Soret-Dufour theory for thermal analysis, was also part of this physical problem. The impact of magnetic fields was also incorporated. A higher temperature distribution was observed in cases of constant wall temperature (CWT) as compared to varying surface temperatures (PST). The temperature distribution increased with an increase in Dufour and Soret numbers, while a reduction in temperature profile was observed with an increasing trend in the Prandtl number. Stress relaxation in viscoelastic fluids increases as the Maxwell parameter increases in value. This causes the liquid to become more solid-like, reducing fluid mobility. The Deborah number, in high magnitude, reduced the flow field of Maxwell fluid.

The present study has provided valuable insights into the behaviour of Maxwell fluids around a rotating and stretching cylinder using Soret and Dufour effects, demonstrating the effects of various parameters on the fluid flow and heat transfer characteristics. However, there remain several unexplored research directions for further investigation. In future, one may explore different boundary conditions to further understand how these conditions impact heat transmission and flow patterns and boundary layer flow around rotating and stretching cylinder. Moreover, heat transportation under the Soret-Dufour effect with the bioconvection phenomenon for different fluid models can also be investigated.

References

- [1].Crane, L. J. (1975). Boundary layer flow due to a stretching cylinder. *Zeitschrift für angewandte Mathematik und Physik ZAMP*, 26(5), 619-622..
- [2]. Wang, C. Y. (1989). Free convection on a vertical stretching surface. *ZAMM-Journal of Applied Mathematics and Mechanics/Zeitschrift für Angewandte Mathematik und Mechanik*, 69(11), 418-420..
- [3].Dandapat, B. S., & Gupta, A. S. (1989). Flow and heat transfer in a viscoelastic fluid over a stretching sheet. *International Journal of Non-Linear Mechanics*, 24(3), 215-219.
- [4].Vajravelu, K. (2001). Viscous flow over a nonlinearly stretching sheet. *Applied mathematics and computation*, 124(3), 281-288.
- [5].Fang, T., & Yao, S. (2011). Viscous swirling flow over a stretching cylinder. *Chinese Physics Letters*, 28(11), 114702.
- [6].Tsou, F. K., Sparrow, E. M., & Goldstein, R. J. (1967). Flow and heat transfer in the boundary layer on a continuous moving surface. *International Journal of Heat and Mass Transfer*, 10(2), 219-235.
- [7]. Sprague, M. A., & Weidman, P. D. (2010). Three-dimensional flow induced by the torsional motion of a cylinder. *Fluid Dynamics Research*, 43(1), 015501.
- [8]. Mukhopadhyay, S. (2013). MHD boundary layer flow and heat transfer over an exponentially stretching sheet embedded in a thermally stratified medium. *Alexandria Engineering Journal*, 52(3), 259-265.
- [9]. Takhar, H. S., Chamkha, A. J., & Nath, G. (2003). Flow and heat transfer on a stretching surface in a rotating fluid with a magnetic field. *International journal of thermal sciences*, 42(1), 23-31..
- [10].Mahmood, T., Ali, S., & Khan, A. (2020). Magnetohydrodynamic flow due to a stretching surface in rotating fluid. *Punjab University Journal of Mathematics*, 46(1).
- [11]. Khan, M., Ahmed, J., & Ahmad, L. (2018). Chemically reactive and radiative von Kármán swirling flow due to a rotating disk. *Applied Mathematics and Mechanics*, 39, 1295-1310.
- [12].Murtaza, M. G., Ferdows, M., Misra, J. C., & Tzirtzilakis, E. E. (2019). Three-dimensional biomagnetic Maxwell fluid flow over a stretching surface in presence of heat source/sink. *International Journal of Biomathematics*, 12(03), 1950036.

- [13]. Ahmed, J., Khan, M., & Ahmad, L. (2019). Transient thin film flow of nonlinear radiative Maxwell nanofluid over a rotating disk. *Physics Letters A*, 383(12), 1300-1305.
- [14]. Wang, C. Y. (1988). Stretching a surface in a rotating fluid. *Zeitschrift für angewandte Mathematik und Physik ZAMP*, 39(2), 177-185.
- [15]. Waqas, H., Imran, M., Khan, S. U., Shehzad, S. A., & Meraj, M. A. (2019). Slip flow of Maxwell viscoelasticity-based micropolar nanoparticles with porous medium: a numerical study. *Applied Mathematics and Mechanics*, 40, 1255-1268.
- [16]. Rehman, K. U., Khan, A. U., Rehman, F., & Shatanawi, W. (2022). Thermal case study on linearly twisting cylinder: a radial stagnation point flow of nanofluid. *Case Studies in Thermal Engineering*, 31, 101861..
- [17]. Choi, J. J., Rusak, Z., & Tichy, J. A. (1999). Maxwell fluid suction flow in a channel. *Journal of non-newtonian fluid mechanics*, 85(2-3), 165-187.
- [18]. Ahmed, J., Khan, M., & Ahmad, L. (2019). MHD swirling flow and heat transfer in Maxwell fluid driven by two coaxially rotating disks with variable thermal conductivity. *Chinese Journal of Physics*, 60, 22-34.
- [19]. Seddeek, M. A., & Abdelmeguid, M. S. (2006). Effects of radiation and thermal diffusivity on heat transfer over a stretching surface with variable heat flux. *Physics Letters A*, 348(3-6), 172-179.
- [20]. Salleh, M. Z., Nazar, R., & Pop, I. (2010). Boundary layer flow and heat transfer over a stretching sheet with Newtonian heating. *Journal of the Taiwan Institute of Chemical Engineers*, 41(6), 651-655.
- [21]. Mahapatra, T. R., & Gupta, A. S. (2002). Heat transfer in stagnation-point flow towards a stretching sheet. *Heat and Mass transfer*, 38(6), 517-521.
- [22]. Picchi, D., Poesio, P., Ullmann, A., & Brauner, N. (2017). Characteristics of stratified flows of Newtonian/non-Newtonian shear-thinning fluids. *International Journal of Multiphase Flow*, 97, 109-133.
- [23]. Gangadhar, K., Venkata Subba Rao, M., & Sobhana Babu, P. R. (2021). Numerical analysis for steady boundary layer flow of Maxwell fluid over a stretching surface embedded in a porous medium with viscous dissipation using the spectral relaxation method. *International Journal of Ambient Energy*, 42(13), 1492-1498.
- [24]. Madhu, M., Kishan, N., & Chamkha, A. J. (2017). Unsteady flow of a Maxwell nanofluid over a stretching surface in the presence of magnetohydrodynamic and thermal radiation effects. *Propulsion and Power research*, 6(1), 31-40.

- [25]. Javed, M. F., Khan, M. I., Khan, N. B., Muhammad, R., Rehman, M. U., Khan, S. W., & Khan, T. A. (2018). Axisymmetric flow of Casson fluid by a swirling cylinder. *Results in Physics*, 9, 1250-1255.
- [26]. Weidman, P. (2019). Radial stagnation flow on a twisting cylinder. *Journal of Fluids Engineering*, 141(11), 114502.
- [27]. Mabood, F., Imtiaz, M., Alsaedi, A., & Hayat, T. (2016). Unsteady convective boundary layer flow of Maxwell fluid with nonlinear thermal radiation: a numerical study. *International Journal of Nonlinear Sciences and Numerical Simulation*, 17(5), 221-229.
- [28]. Al Nuwairan, M., Hafeez, A., Khalid, A., Souayeh, B., Alfadhli, N., & Alnaghmosh, A. (2022). Flow of maxwell fluid with heat transfer through porous medium with thermophoresis particle deposition and Soret–Dufour effects: Numerical solution. *Coatings*, 12(10), 1567.
- [29]. Haritha, A., Devasena, Y., & Vishali, B. (2017). MHD heat and mass transfer of the unsteady flow of a Maxwell fluid over a stretching surface with Navier slip and convective boundary conditions. *Global Journal of Pure and Applied Mathematics*, 13(6), 2169-2179.
- [30]. Abdullah, N. N., Som, A. N. M., Arifin, N. M., & Ab Ghani, A. (2023). The Effect of MHD on Marangoni Boundary Layer of Hybrid Nanofluid Flow Past a Permeable Stretching Surface. *CFD Letters*, 15(5), 65-73.
- [31]. Riaz, M. B., Asgir, M., Zafar, A. A., & Yao, S. (2021). Combined effects of heat and mass transfer on mhd free convective flow of maxwell fluid with variable temperature and concentration. *Mathematical Problems in Engineering*, 2021, 1-36.
- [32]. Khan, W. A., Rashad, A. M., Abdou, M. M. M., & Tlili, I. (2019). Natural bioconvection flow of a nanofluid containing gyrotactic microorganisms about a truncated cone. *European Journal of Mechanics-B/Fluids*, 75, 133-142.
- [33]. Hill, N. A., & Pedley, T. J. (2005). Bioconvection. *Fluid Dynamics Research*, 37(1-2), 1.
- [34]. Kuznetsov, A. V., Avramenko, A. A., & Geng, P. (2003). " Dept. of Mechanical and Aerospace Engineering, North Carolina State University. *Heat Mass Transfer*, 30(5), 593-602.
- [35]. Pedley, T. J., Hill, N. A., & Kessler, J. O. (1988). The growth of bioconvection patterns in a uniform suspension of gyrotactic micro-organisms. *Journal of fluid mechanics*, 195, 223-237.
- [36]. Mariam, A., Siddique, I., Abdal, S., Jarad, F., Ali, R., Salamat, N., & Hussain, S. (2022). Bioconvection attribution for effective thermal transportation of upper convicted Maxwell nanofluid flow due to an extending cylindrical surface. *Case Studies in Thermal Engineering*, 34, 102062.

- [37]. Zhang, L., Puneeth, V., Ijaz Khan, M., El-Zahar, E. R., Manjunath, N., Shah, N. A., ... & Khan, M. I. (2022). Applications of bioconvection for tiny particles due to two concentric cylinders when role of Lorentz force is significant. *Plos one*, *17*(5), e0265026.
- [38]. Bees, M. A., & Hill, N. A. (1998). Linear bioconvection in a suspension of randomly swimming, gyrotactic micro-organisms. *Physics of Fluids*, *10*(8), 1864-1881.
- [39]. Khan, W. A., Rashad, A. M., Abdou, M. M. M., & Tlili, I. (2019). Natural bioconvection flow of a nanofluid containing gyrotactic microorganisms about a truncated cone. *European Journal of Mechanics-B/Fluids*, *75*, 133-142.
- [40]. Saleem, S., Rafiq, H., Al-Qahtani, A., El-Aziz, M. A., Malik, M. Y., & Animasaun, I. L. (2019). Magneto Jeffrey nanofluid bioconvection over a rotating vertical cone due to gyrotactic microorganism. *Mathematical Problems in Engineering*, 2019.
- [41]. Childress, S., Levandowsky, M., & Spiegel, E. A. (1975). Pattern formation in a suspension of swimming microorganisms: equations and stability theory. *Journal of Fluid Mechanics*, *69*(3), 591-613.
- [42]. Kuznetsov, A. V. (2005). Thermo-bioconvection in a suspension of oxytactic bacteria. *International communications in heat and mass transfer*, *32*(8), 991-999.
- [43]. Geng, P., & Kuznetsov, A. V. (2004). Effect of small solid particles on the development of bioconvection plumes. *International communications in heat and mass transfer*, *31*(5), 629-638.
- [44]. Aziz, A., Khan, W. A., & Pop, I. (2012). Free convection boundary layer flow past a horizontal flat plate embedded in porous medium filled by nanofluid containing gyrotactic microorganisms. *International Journal of Thermal Sciences*, *56*, 48-57.
- [45]. Hillesdon, A. J., & Pedley, T. J. (1996). Bioconvection in suspensions of oxytactic bacteria: linear theory. *Journal of Fluid Mechanics*, *324*, 223-259.
- [46]. Zhang, L., Arain, M. B., Bhatti, M. M., Zeeshan, A., & Hal-Sulami, H. (2020). Effects of magnetic Reynolds number on swimming of gyrotactic microorganisms between rotating circular plates filled with nanofluids. *Applied Mathematics and Mechanics*, *41*, 637-654.
- [47]. Al-Khaled, K., Khan, S. U., & Khan, I. (2020). Chemically reactive bioconvection flow of tangent hyperbolic nanoliquid with gyrotactic microorganisms and nonlinear thermal radiation. *Heliyon*, *6*(1).
- [48]. Ghorai, S., & Hill, N. A. (1999). Development and stability of gyrotactic plumes in bioconvection. *Journal of Fluid Mechanics*, *400*, 1-31.

- [49]. Shah, S. A. A., Ahammad, N. A., Din, E. M. T. E., Gamaoun, F., Awan, A. U., & Ali, B. (2022). Bio-convection effects on prandtl hybrid nanofluid flow with chemical reaction and motile microorganism over a stretching sheet. *Nanomaterials*, *12*(13), 2174.
- [50]. Yin, J., Zhang, X., Rehman, M. I. U., & Hamid, A. (2022). Thermal radiation aspect of bioconvection flow of magnetized Sisko nanofluid along a stretching cylinder with swimming microorganisms. *Case Studies in Thermal Engineering*, *30*, 101771.
- [51]. Wang, J., Mustafa, Z., Siddique, I., Ajmal, M., Jaradat, M. M., Rehman, S. U., ... & Ali, H. M. (2022). Computational analysis for bioconvection of microorganisms in prandtl nanofluid darcy–forchheimer flow across an inclined sheet. *Nanomaterials*, *12*(11), 1791.
- [52]. Iqbal, Z., Mehmood, Z., & Maraj, E. N. (2017). Oblique transport of gyrotactic microorganisms and bioconvection nanoparticles with convective mass flux. *Physica E: Low-dimensional Systems and Nanostructures*, *88*, 265-271.
- [53]. Song, Y. Q., Hamid, A., Khan, M. I., Gowda, R. P., Kumar, R. N., Prasannakumara, B. C., ... & Malik, M. Y. (2021). Solar energy aspects of gyrotactic mixed bioconvection flow of nanofluid past a vertical thin moving needle influenced by variable Prandtl number. *Chaos, Solitons & Fractals*, *151*, 111244.
- [54]. Zuhra, S., Khan, N. S., & Islam, S. (2018). Magneto hydrodynamic second-grade nanofluid flow containing nanoparticles and gyrotactic microorganisms. *Computational and Applied Mathematics*, *37*, 6332-6358.
- [55]. Hopkins, M. M., & Fauci, L. J. (2002). A computational model of the collective fluid dynamics of motile micro-organisms. *Journal of Fluid Mechanics*, *455*, 149-174.
- [56]. Khan, A., Saeed, A., Tassaddiq, A., Gul, T., Mukhtar, S., Kumam, P., ... & Kumam, W. (2021). Bio-convective micropolar nanofluid flow over thin moving needle subject to Arrhenius activation energy, viscous dissipation and binary chemical reaction. *Case Studies in Thermal Engineering*, *25*, 100989.
- [57]. Ali, B., Ali, M., Hussain, S., Yahya, A. U., & Hussain, I. (2022). Tangent hyperbolic nanofluid: Significance of Lorentz and buoyancy forces on dynamics of bioconvection flow of rotating sphere via finite element simulation. *Chinese Journal of Physics*, *77*, 658-671.
- [58]. Rashad, A. M., & Nabwey, H. A. (2019). Gyrotactic mixed bioconvection flow of a nanofluid past a circular cylinder with convective boundary condition. *Journal of the Taiwan Institute of Chemical Engineers*, *99*, 9-17.
- [59]. Mallikarjuna, B., Rashad, A. M., Chamkha, A., & Abdou, M. M. M. (2018). Mixed bioconvection flow of a nanofluid containing gyrotactic microorganisms past a vertical slender cylinder. *Frontiers in Heat and Mass Transfer (FHMT)*, *10*.

- [60]. Ishikawa, T. (2009). Suspension biomechanics of swimming microbes. *Journal of The Royal Society Interface*, 6(39), 815-834.
- [61]. Khan, U., Ahmed, N., & Mohyud-Din, S. T. (2016). Influence of viscous dissipation and Joule heating on MHD bio-convection flow over a porous wedge in the presence of nanoparticles and gyrotactic microorganisms. *Springerplus*, 5, 1-18.
- [62]. Kim, J., Kang, Y. T., & Choi, C. K. (2007). Soret and Dufour effects on convective instabilities in binary nanofluids for absorption application. *International journal of refrigeration*, 30(2), 323-328.
- [63]. Ahmed, A., Khan, M., & Ahmed, J. (2020). Thermal analysis in swirl motion of Maxwell nanofluid over a rotating circular cylinder. *Applied Mathematics and Mechanics*, 41, 1417-1430.
- [64]. Spurk, J., & Aksel, N. (2007). *Fluid mechanics*. Springer Science & Business Media.
- [65]. https://guava.physics.uiuc.edu/~nigel/courses/569/Essays_Fall2007/files/Hu.pdf
- [66]. T. Papanastasiou, G. Georgiou, and A. N. Alexandrou, *Viscous Fluid Flow*. CRC press, pp. 456, 1999
- [67]. White, F. M. (1990). *Fluid mechanics*. New York.